The Modulation of Dynamic Ankle Stiffness with Postural Sway During Upright Stance

Christopher B. Lang

Master of Engineering

Biomedical Engineering

McGill University
Montreal, Quebec
2014-04-15

A thesis submitted to McGill University in partial fulfillment of the requirements of the degree of M.Eng in Biomedical Engineering.

© Christopher Lang, 2014

ACKNOWLEDGEMENTS

I would like to thank my supervisor, Dr. Robert Kearney, for patiently guiding my studies and for helping to focus my research at times when I "rode madly off in all directions". I would also like to thank my labmates, who helped to create a pleasant working atmosphere at the REKLAB and who were eager to help with experiments and offer suggestions. I would furthermore like to thank my family for their consistent support and encouragement, and my friends for their positivity and diversions outside of the lab. This work was funded by the Canadian Institutes of Health Research (CIHR).

ABSTRACT

Ankle stiffness is a nonlinear, time-varying system which contributes to the control of human upright stance. This study examined the nature of the contribution of stiffness to postural control by determining how intrinsic and reflex stiffnesses vary with sway. Subjects were instructed to stand quietly on a bilateral electro-hydraulic actuator while position perturbations were applied about the ankle. Subjects performed three types of trials: normal stance, forward lean, and backward lean. Position, torque, and EMGs from the tibialis anterior and triceps surae muscles were recorded. Background torque, intrinsic stiffness and reflex stiffness were calculated for each perturbation. Intrinsic and reflex stiffnesses were heavily modulated by postural sway. Moreover, they were modulated in a complimentary manner; intrinsic stiffness was lowest when reflex gain was highest, and vice versa. These findings suggest that intrinsic stiffness is modulated simultaneously with reflex stiffness to optimize the control of balance.

ABRÉGÉ

La phnomne de raideur au niveau de la cheville est un systme non linaire et variant dans le temps qui contribue au contrle de la position debout chez l'humain. Cette tude a examin la nature de la contribution de la raideur sur le contrle postural en dterminant comment la rigidit intrinsque ainsi que les rflexes varient selon le ballant. Les sujets ont t chargs de se tenir tranquillement sur un actionneur lectrohydraulique bilatral tandis que des perturbations de position ont t appliques sur la cheville. Les sujets ont effectus trois types d'essais : posture normal, inclin vers l'avant et puis vers l'arrire. La position, le moment de force ainsi que l'EMG du muscle tibial antrieur et triceps surae ont t enregistres en continu. Le moment de base, la raideur et la rigidit intrinsque du rflexe ont t calculs pour chaque perturbation. La rigidit intrinsque et rflexe ont t fortement moduls par le balancement postural. De plus, ils ont t moduls de manire complmentaire; la rigidit intrinsque est la plus faible lorsque le gain en rflexe tait le plus leve et vice versa. Ces rsultats suggrent que la rigidit intrinsque est module en mme temps que la rigidit rflexe afin d'optimiser le contrle de l'quilibre.

TABLE OF CONTENTS

ACK	NOWI	LEDGEMENTS ii
ABS	TRAC	Γ
ABR	ÉGÉ	
LIST	OF T	ABLES viii
LIST	OF F	IGURES ix
1	Introd	uction
	1.1 1.2	Thesis Objectives
2	Literat	ture Review
	2.12.22.32.42.5	Ankle Anatomy and Physiology 2.1.1 Musculoskeletal Anatomy 2.1.2 The Muscle Spindle 2.1.3 The Golgi Tendon Organ 8 Standing Dynamics and Mechanical Model 2.2.1 Postural Sway 2.2.2 Modeling Upright Stance Postural Control 2.3.1 Passive Control 2.3.2 Active Control 3 Joint Stiffness 27 2.4.1 Modulation of Joint Stiffness 27 2.4.2 Measurement and Identification of Joint Stiffness 36 Rationale 35
3	Experi	imental Methods

	3.1	Experimental Apparatus
		3.1.1 Bilateral Hydraulic Actuator
		3.1.2 Safety Mechanisms
		3.1.3 Sensors
		3.1.4 Data Acquisition and Experimental Control
	3.2	Experimental Paradigms
		3.2.1 Subject Preparation
		3.2.2 Trial Types and Execution
		3.2.3 Input Signal
4	System	n Identification Methods and Non-Results
	4.1	Parallel Cascade Identification - Full Record
	1.1	4.1.1 Methods
		4.1.2 Results
	4.2	Parallel Cascade Identification - Short Segments
		4.2.1 Methods
		4.2.2 Results
	4.3	Conclusion
5	Indivi	dual Response Processing and Analysis
	5.1	Methods
	5.2	Results
		5.2.1 Intrinsic Stiffness
		5.2.2 Reflex Stiffness
		5.2.3 EMG Variation
		5.2.4 Covariation of Intrinsic and Reflex Stiffnesses 82
		5.2.5 Feedforward Control
	5.3	Summary
6	Discus	ssion and Conclusions
	6.1	Modulation of Ankle Stiffness
	6.2	Limitations
		6.2.1 Variability
	6.3	Future Work
		6.3.1 Modulation of Stiffness
		6.3.2 System Identification
		6.3.3 Contralateral Mechanisms

	6.3.4 Sensory Contributions to Stiffness	93
6.4	Conclusions	93
References		95

LIST OF TABLES

Table		page
3-1	Signals collected	. 43
3-2	Gender, age, height, and weight for each subject	. 45
5-1	Height, weight, and K_{crit} for each subject	. 68
6-1	Maximum Intrinsic Stiffness $\left(\frac{K}{K_{crit}}\right)$. 88

LIST OF FIGURES

Figure		page
2-1	Bones associated with the articulation of the ankle joint [62]	4
2-2	Muscles of the lower leg [2]	6
2-3	Muscle spindle organ and associated neural pathways [40]	7
2-4	Single inverted pendulum model [46]	10
2-5	A general model of postural control. The CNS maintains postural stability by altering active muscle stiffness, based on sensory feedback. Some pathways may also generate torques by mechanisms which are not directly related to joint stiffness. The dotted lines represent connections whose models and contributions are uncertain.	. 15
2-6	Parallel-cascade model of joint stiffness. Sample signals are shown in blue, modeled responses in red, non-parametric derived descriptions in orange and parametric fits to the non-parametric models in green. Intrinsic stiffness is estimated with a linear second order IRF in the upper pathway, while a Hammerstein system receiving velocity as an input models the reflex activity [41]	33
3-1	Bilateral hydraulic actuator with primary components labeled	38
3-2	Foot pedal assembly with load cell positions indicated [55]	41
3-3	Diagram of the electronics setup for experimental data acquisition [55].	. 44
3–4	Axis of rotation of the talocrural joint as measured from ankle anatomical landmarks [22]	46
3-5	Ten seconds of a typical PRBS signal recorded from the potentiometer	. 49
3-6	Cross-correlation between left and right input PRBS signals for a typical trial	49

Sample fit for the parallel cascade method used on a supine experimental data (left) and upright stance experimental data (right), with residuals shown in the lower panels. The supine fitting achieved a 92% VAF while the upright stance fitting yielded a 44% VAF	52
Power spectrum of the residuals from a parallel cascade fitting	52
Low-frequency power for torque from a sample quiet stance experiment (top) and bilateral experiment (bottom). The reflexes generated in an experiment add low-frequency power to the spectrum	53
Sample calculations of sway torque collected from experiments without perturbations. The residuals shown are for the 1 Hz filter	54
Sample calculations of sway torque for experiments performed in the resting supine condition (left) and in upright stance (right)	55
Sample background torque (sway torque) with segments and background EMG (raw EMG signal low-pass filtered at 1 Hz with reflex EMG removed) for a bilaterally perturbed experiment	59
Parallel cascade identification performed on 12 seconds of experimental data. This example achieved a VAF of 85%	60
Identified Hammerstein system for the previously shown segment of data	61
Sample spike detections for pedal velocity. Pedal position is normalized between -1 and 1. The onsets shown are the time values identified by the spike detection algorithm	63
Sample subdivided response drawn from a typical experiment. Position is normalized between -5 and 5, and EMG is rectified and normalized between -30 and -15. Peak detected velocity occurs at 50ms. The subsections are as follows: (A) pre-response (0-25ms), (B) intrinsic response (25-100ms), (C) reflex response (100-350ms), (D) post-reflex (350-500ms)	64
Typical IBK model fit to intrinsic torque of a single response. The beginning of the reflex response can be observed toward the end of the window	66
	tal data (left) and upright stance experimental data (right), with residuals shown in the lower panels. The supine fitting achieved a 92% VAF while the upright stance fitting yielded a 44% VAF Power spectrum of the residuals from a parallel cascade fitting Low-frequency power for torque from a sample quiet stance experiment (top) and bilateral experiment (bottom). The reflexes generated in an experiment add low-frequency power to the spectrum Sample calculations of sway torque collected from experiments without perturbations. The residuals shown are for the 1 Hz filter Sample calculations of sway torque for experiments performed in the resting supine condition (left) and in upright stance (right) Sample background torque (sway torque) with segments and background EMG (raw EMG signal low-pass filtered at 1 Hz with reflex EMG removed) for a bilaterally perturbed experiment Parallel cascade identification performed on 12 seconds of experimental data. This example achieved a VAF of 85%

5-4	Background torque, intrinsic, and reflex fitting for one sample response. The "Trend" line represents the background torques computed from each subsection added to the simulated intrinsic torque based on the estimated intrinsic stiffness value 'K'	67
5-5	Sample reflex fits for strong and weak responses	67
5–6	Raw data from a forward-leaning trial showing pedal position, torque, and rectified EMG. A positive position indicates a dorsiflexing perturbation, while a negative position indicates a plantarflexing perturbation. Positive torque signified that the subject's weight was centered closer to their heels, while negative torque signified that the subject's weight was centered closer to their toes	71
5–7	Ten individual responses taken from different background torques. Ten groups of equal width in background torque are shown, and a single response was plotted from each group. Group 1 represents the responses with the lowest background torque while group 10 contains the responses with the largest background torque. The background torque value was subtracted from the torque response.	72
5–8	Intrinsic stiffness values for all responses from the left leg of subjects 1-5, with a trend line is shown in red. The stiffness is shown as a percentage of the critical value, which was calculated according to Equation 2.3. The green dots represent responses from the normal trial paradigm, while the blue dots represent responses from the leaning trials	73
5–9	Intrinsic stiffness values for all responses from the left leg of subjects 6-9, with a trend line is shown in red. The stiffness is shown as a percentage of the critical value, which was calculated according to Equation 2.3. The green dots represent responses from the normal trial paradigm, while the blue dots represent responses from the leaning trials	74
5-10	Intrinsic stiffness trends superimposed for all subjects. The mean background torque of the trend line was subtracted for each subject. Positive torque signified that the subject's weight was centered closer to their heels, while negative torque signified that the subject's weight was centered closer to their toes	75

5–11 Parameter variance estimates for one subject. The standard error of the fitted parameter 'K' is shown for each point. The "Fit +/- Standard Error" lines show the standard error values passed through an averaging filter, then added to and subtracted from the moving window median fit.	76
5–12 Reflex gains for all responses from the left leg of all reflex-displaying subjects. The value of the trend line is the median of the reflex gains of the responses within 5 Nm background torque. The green dots represent responses from the normal trial paradigm, while the blue dots represent responses from the leaning trials	78
5–13 Moving window median of reflex gain for subjects exhibiting consistent reflex responses. The mean background torque was subtracted for each subject	79
5–14	80
5–15 Sample distribution of torque versus background muscle activation. Data includes all leaning trials in addition to two normal trials	81
5–16 EMG activation trends for all subjects for all muscles in leaning bilaterally perturbed trials. EMG for each subject is normalized from 0 to 1 based on the minimum and maximum background activation observed from the collection of all perturbation responses.	83
5–17 Critical stiffness (left/black axis) and reflex gain (right/red axis) superimposed for both legs of the five subjects who displayed reflexes. The curves shown are the moving window median trends displayed in previous sections	84
5–18 Distribution of intrinsic and reflex stiffness versus sway velocity for the left leg of a typical subject. Each blue dot represents one individual response	8F

CHAPTER 1 Introduction

The maintenance of balance in humans is the result of interactions between neural control mechanisms and body dynamics. The task of maintaining balance, and the systems involved, are complex. It is a widely studied and narrowly understood subject. The control task is inherently difficult; it resembles the task of stabilizing an inverted pendulum, since humans must maintain a large mass steady over a relatively narrow base of support.

Dynamic ankle stiffness, which describes the relationship between the position of the ankle and the torque generated about it, contributes to the stabilization of this pendulum. A major cause for difficulty in understanding joint stiffness is the highly variable nature of biological systems. In the case of upright stance, there is evidence that ankle position and contraction level modulate ankle stiffness. Additionally, the central nervous system can both generate torque and alter joint stiffness by integrating information from the visual, vestibular, and proprioceptive systems. While these inputs are understood to affect stiffness, the exact manner in which they do is unclear. These issues subsequently create difficulty in identifying a system model, as many identification methods are not designed to account for the complex structure or time-varying behavior of the postural control system. Despite these challenges, the applications of joint stiffness research are numerous. There is potential to use joint stiffness to characterize neuromuscular deficits by comparing pathological stiffness to

normal values. Such information could be used to design more effective rehabilitation procedures and could improve the development and design of assistive robotics used to restore function to a joint.

1.1 Thesis Objectives

The research presented herein examines the contribution of ankle stiffness to stance control and how stiffness varies with postural sway observed during quasi-static postural leans. Intrinsic and reflex stiffness will be evaluated and compared to measures that define the postural state in an attempt to measure the time-varying dynamics of stiffness.

1.2 Outline of Thesis

This thesis is divided into 5 chapters. Chapter 1 gives a brief outline of the current state of research for the study of ankle stiffness and postural control and summarizes the goals of the research project.

Chapter 2 presents a literature review of topics relevant to the project. This includes a discussion of ankle anatomy and stretch reflex physiology, an overview of standing dynamics and postural control, and a review of how joint stiffness is estimated.

Chapter 3 includes a description of the experimental apparatus, sensors used, signals collected, trial paradigms, and data analysis methods.

Chapter 4 presents the experimental results, and describes how intrinsic and reflex stiffness at the ankle vary with postural sway observed during quasi-static postural leans.

Chapter 5 discusses the findings presented in the previous chapter and their implications for the study of postural control. It also describes the limitations of the research and provides some suggestions for future research.

CHAPTER 2 Literature Review

2.1 Ankle Anatomy and Physiology

Maintaining balance requires the coordinated activity of leg muscles to generate an appropriate torque to stabilize the mass of the body. Voluntary and involuntary contractile mechanisms of these muscles act through the skeletal system to maintain an upright position.

2.1.1 Musculoskeletal Anatomy

The ankle joint is a synovial hinge joint whose articular surfaces include the distal ends of the tibia and fibula and the superior part of the talus [44], as shown in Figure 2–1. The distal ends of the tibia and fibula form the *malleolar mortise*, a socket into which the rounded superior surface of the talus fits [44].



Figure 2–1: Bones associated with the articulation of the ankle joint [62].

The hinge joint classification befits the ankle, since it moves primarily about one axis. Plantarflexion of the ankle is defined as a downward rotation of the ankle joint toward the plantar surface (sole) of the foot. The ankle can be plantarflexed approximately 50° from the neutral position. Dorsiflexion describes the opposite motion: the rotation of the joint toward the dorsal surface of the foot to a maximum of about 20°. The range of motion of the ankle is limited by passive resistance from muscle stretch and tension in the surrounding ligaments [44]. About the subtalar joint, the ankle can also experience inversion and eversion, which move the sole either toward or away from the medial plane, respectively [44].

The main muscles contributing to the movement of the ankle are the tibialis anterior (TA) and the triceps surae (TS) group of muscles: the medial and lateral heads of the gastrocnemius (GS) muscle and the soleus muscle. These are illustrated in Figure 2–2. The TA is the primary ankle dorsiflexor, and the soleus and GS muscles are the main contributors to ankle plantarflexion, which is approximately four times stronger than dorsiflexion [44]. The soleus is located deep to the GS muscle, and is composed primarily of slow-twitch fibers. This makes it well-suited for continuously opposing the effects of gravity, as it is capable of sustained contraction, which is evidenced by electromyographic studies showing its continuous activity during standing [44]. The GS muscles are superficial ankle plantarflexors, composed mostly of fast-twitch fibers. Thus, this muscle is well-suited for rapid, powerful contractions that are required during running and jumping, and acts only intermittently during standing [44]. The GS functions most effectively when the knee is extended and the ankle is in a dorsiflexed position; it cannot produce plantarflexion when the knee is fully

flexed since its origin of attachment is above the knee joint [44]. These muscles work together to stabilize the mass of the standing human.

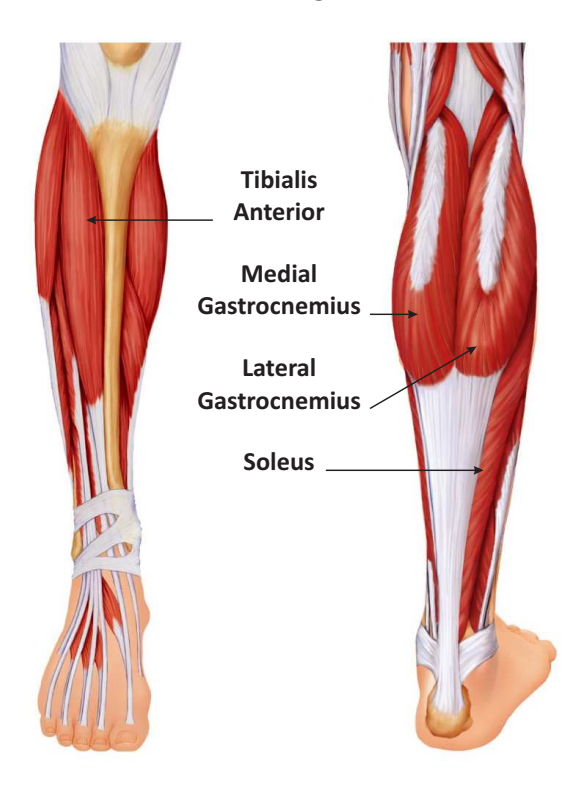


Figure 2–2: Muscles of the lower leg [2].

2.1.2 The Muscle Spindle

The central nervous system controls posture in part through the use of information received by receptors located within muscle fibers. Muscle fibers can be divided into two types: intrafusal and extrafusal. The extrafusal fibers are responsible for the main generation of force for a muscle, while the intrafusal component (composed of nuclear chain fibers and nuclear bag fibers) is primarily responsible for sensing changes in muscle fiber length and velocity and relaying such information to the central nervous system. Groups of these intrafusal fibers form muscle spindles (shown in Figure 2–3), the main feedback sensor in the belly of the muscle [56].

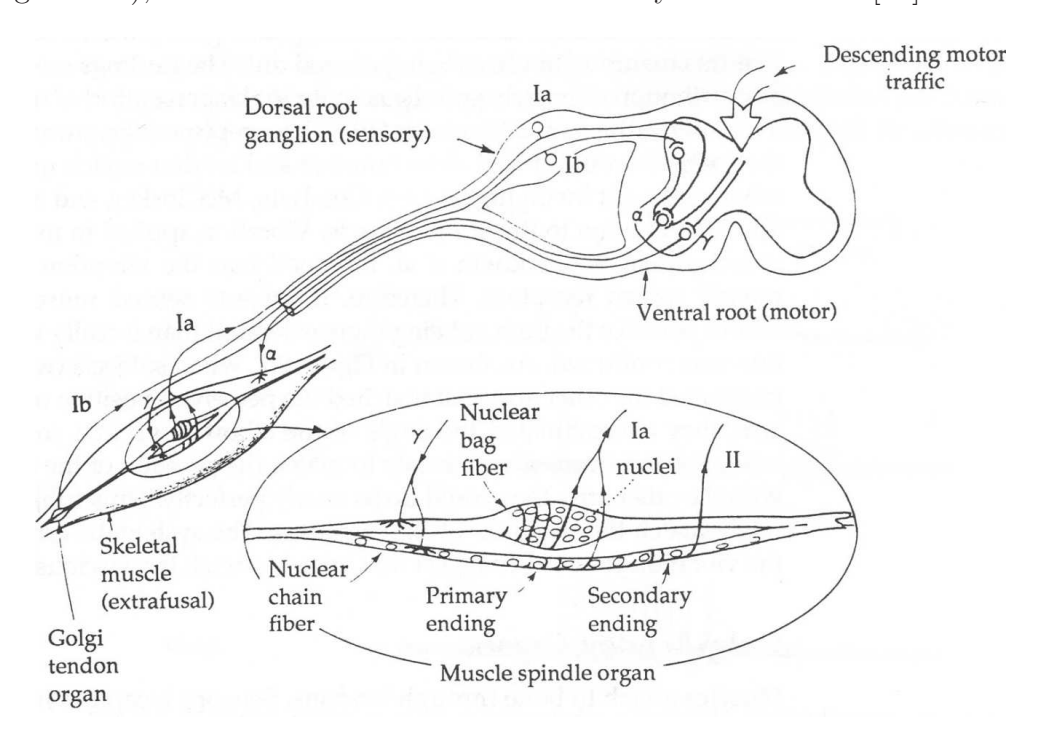


Figure 2–3: Muscle spindle organ and associated neural pathways [40].

Several neural pathways use signals received from different parts of the spindle organ to transmit information to the central nervous system. The Ia sensory nerve is wrapped around the central region of the spindle. Differences in extrafusal and intrafusal fiber length, as well as stretch velocity of the intrafusal fibers, cause firing of the Ia afferent. This results in the excitation of the alpha motor neuron in the spinal cord, causing a subsequent muscle contraction. This, in turn, lowers the overall stretch on the spindle. As the amplitude of the stretch increases, so does the firing rate of the muscle spindle [59]. After relief of the stretch, the Ia firing

rate slows and the reflex contraction subsides [56]. Ia afferent neurons also connect polysynaptically, connecting with interneurons that innervate antagonist muscles and inhibit alpha motor neuron firing. This process is referred to as reciprocal inhibition [58], and reduces the contraction level and tension in the muscle.

The group II afferent nerve generally responds only to static stretching of muscle fibers, although in some cases can exhibit more dynamic sensitivity [21]. Its firing rate increases proportionally to the length of the muscle and, unlike the Ia afferent, the group II nerve is insensitive to rapid stretches [18].

The dynamics of the muscle spindle are additionally affected by gamma motor neurons, which innervate the contractile fibers at either end of the spindle. When an alpha neuron fires, the intrafusal fibers will shorten along with the extrafusal fiber. This reduction in length reduces the stretch sensitivity. To offset this effect, gamma neurons fire simultaneously with the alpha motor neurons; this is referred to as alpha-gamma coactivation. This causes the contractile end regions of the intrafusal fibers to shorten, creating a lengthening of the sensory portions in the interior region, balancing the passive shortening caused by the extrafusal contraction. This adaptive mechanism allows the muscle spindle to maintain the same sensitivity to stretch throughout a muscle contraction [58, 59].

2.1.3 The Golgi Tendon Organ

The Golgi tendon organ is a sensory organ that resides inside muscle tendons. In contrast with the muscle spindle, the Golgi organ is more sensitive to muscle tension [24]. When the contraction level increases, the firing rate of the Golgi tendon organ increases, sending a signal that causes a reduction in muscle tension [56].

2.2 Standing Dynamics and Mechanical Model

The maintenance of upright stance is inherently difficult. To remain upright, humans must regulate the position of their center of mass (COM) such that their center of pressure (COP) remains within the base of support. This is done through the exertion of corrective torques by the feet against the support surface to counteract the tendency of gravity to accelerate the body away from an equilibrium position [52]. The task is complicated by the fact that the mass of the body is large and must be stabilized over a small base of support.

2.2.1 Postural Sway

During quiet stance, there is a low frequency, random variation in the ankle torque that persists in experiments in which perturbations are applied. This phenomenon will hereon be referred to as sway torque, or background torque, and reflects the quasi-random motion of the COP during upright stance. This sway is characterized by a tight coupling of COP motion to the activation of ankle plantarflexors for each leg and a high correlation of COP motion between the left and right feet [43]. Additionally, there is evidence for interlimb coordination of postural sway, as evidenced by a common bilateral modulation of the soleus activities during postural tasks. This modulation is weaker for voluntary tasks, suggesting that sway patterns change and different control strategies are employed as the task requirements vary [43]. Sway can additionally be affected by voluntary contraction or the use of an ankle orthosis [67].

2.2.2 Modeling Upright Stance

The mechanics of standing in humans are typically simplified and modeled as a single inverted pendulum (SIP), reducing the complexity of the multi-joint system by fixing the angles of the knee and hip joints. The mass of the body is considered to be a point mass at a distance 'h' above the ankle joint, as Figure 2–4 shows. The ankle torque τ_{ankle} is generated by a spring and damper in relation to the joint angle θ . This model is used frequently in the literature [7, 11, 33, 34, 35, 71, 73].

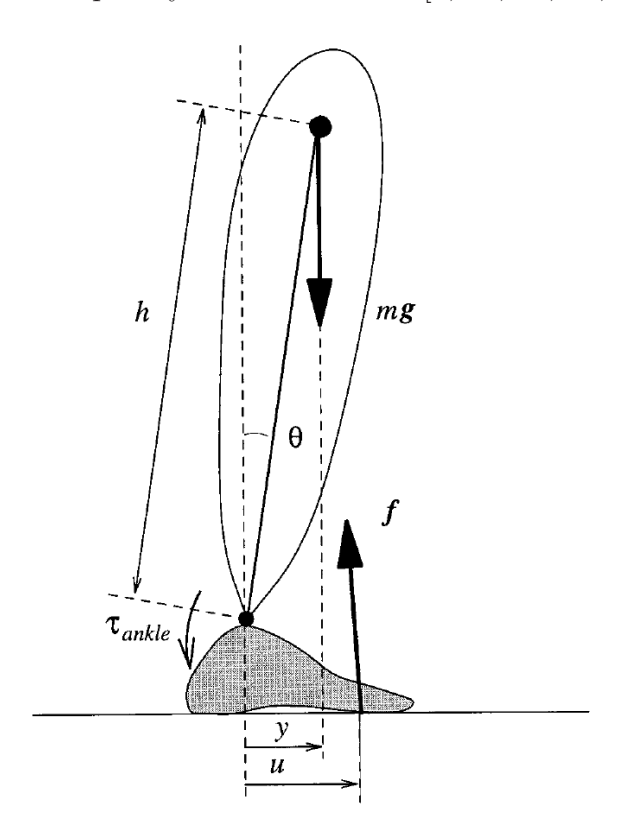


Figure 2–4: Single inverted pendulum model [46].

A core concept to the SIP model is that of a critical stiffness (derived below in Equation 2.3), or K_{crit} . This is the minimum stiffness necessary to prevent the fall of

the inverted pendulum, assuming the angle θ is small. If the stiffness is below K_{crit} , active compensatory mechanisms are required to maintain stability [7].

For the simple inverted pendulum shown in Figure 2–4, the force balance equation is

$$I\ddot{\theta} = \sum M \tag{2.1}$$

$$I\ddot{\theta} = -m \cdot g \cdot h \cdot \sin(\theta) + \tau_{ankle} + M_{ext}$$
 (2.2)

for moment of inertia I, subject mass m, gravitational constant g, COM height h, ankle torque τ_{ankle} , and external moments M_{ext} . For the case of static equilibrium, we assume the acceleration of the COM is negligible ($\ddot{\theta}=0$), external forces are nonexistent ($M_{ext}=0$), and the small angle approximation $sin(\theta)=\theta$ is valid. If it is assumed that passive ankle torque is generated by a spring, $\tau_{ankle}=K\theta$, Equation 2.2 then simplifies to Equation 2.3, which defines the value of critical stiffness.

$$K_{crit} = m \cdot g \cdot h \tag{2.3}$$

The height of the center of mass can be approximated by Equation 2.4, which models the location of the COM [1], for subject height h_{sub} .

$$h = 0.01 \cdot (-48.6 \cdot h_{sub} - 0.0301 \cdot m - 4.775) \tag{2.4}$$

Some research groups support the idea of a more complex model, arguing that the multiple body segment dynamics of standing are not accurately described by a SIP model [16]. Gunther et al. studied subjects during quiet stance, collecting bilateral force platform data, joint angles from cameras, and using inverse dynamic calculations to estimate joint torques. Knee and ankle joint torques varied in phase, while the ankle and hip moved out of phase. These observations supported a multisegment view and countered the SIP model which would predict that the ankle and hip joints would move in-phase [16]. They also asserted that, if the SIP model was valid, the COM, COP and their sum should all have power spectra with a single peak at the same frequency. This was violated by their experimental data that showed spectra with multiple peaks at different frequencies. Simulations of a double-inverted (DIP) pendulum model explained their data better than the SIP model. [17]. A triple-inverted pendulum (TIP) was also suggested as a possibility, although a DIP may be sufficient in most cases, since the knee often acts in concert with the ankle [16, 17].

Creath et al. also support the use of a DIP model [8]. They showed that humans do not control balance using ankle or hip torques exclusively, but consistently use both joints continuously while standing. Contributions from one joint might dominate, however both were always present, which violated the SIP assumption that all torques are generated about the ankle. This, along with the anti-phase relationships observed between trunk and leg segment angles, supports the validity of the DIP model [8].

Warnica et al. tested subjects in quiet stance during several levels of voluntary contraction of the ankle plantarflexors which were insufficient to lift the heels off the ground [67]. Both sway amplitude and the difference between ankle and sway angle increased with increasing levels of voluntary contraction, suggesting more movement occurred about the hip. This suggests that, at higher levels of voluntary contraction, the body behaves less like a SIP [67].

Conversely, Gage et al. presented evidence in support of the SIP model for quiet stance [14]. They showed that ankle angular displacement was highly correlated with motion of the COM, which is consistent with the assumption of a SIP model [14]. Furthermore, in another study, when subjects stood in a side-by-side configuration, anterio-posterior balance was almost completely regulated by the ankle plantarflexors and dorsiflexors [75], as the SIP model would predict. Further support came from subsequent findings that the experimental COP-COM error signal was highly correlated with the horizontal acceleration of the COM. This is consistent with the mechanical model of the inverted pendulum [71].

Overall, the SIP model performs well providing that perturbations to balance are small. The high correlation between ankle activity and the motion of the COM suggests that ankle torque explains the majority of the dynamics of upright stance. This assumes that any instabilities caused by perturbations are not large enough to evoke a significant hip response or a step, conditions which violate the single-joint assumption of the SIP model.

2.3 Postural Control

Different control strategies are employed in upright stance depending on what is mechanically required to maintain balance at any moment. Whenever any stabilizing torque primarily results from contractions of the ankle flexors and extensors, an ankle strategy is said to be in effect. The assumptions of the SIP model are supported when this is the main stabilizing strategy used. This method of stabilization works mainly by repositioning the COP, and is most effective with rigid support surfaces and displacement distances which are short relative to the length of the foot [20].

The ankle strategy is observed during the application of low amplitude, low velocity perturbations [8].

When the COM exceeds a threshold value of displacement or velocity, motion of the hip may be employed, corresponding to dynamics that could be observed in a DIP model. This generates a horizontal shear force against the base of support, and is effective on a non-slippery surface [20]. This strategy is more likely to be employed in response to larger perturbations [8, 51] or when the base of support decreases in size [20]. Finally, if the hip and ankle strategies are insufficient to stabilize the body, a step may be taken to reestablish the COP under the COM [20].

Stable upright stance is thought to be maintained by a combination of ankle and hip strategies, sometimes resulting in hybrid strategies. Early experiments postulated that balance could be achieved by utilizing each strategy individually [20]. Later, Creath et al. showed that these strategies are "co-existing excitable modes" which are always present, although one or the other may dominate at any time [8]. Park et al. reached a similar conclusion and showed that hip gains increase and ankle gains decrease nearly linearly with perturbation amplitude [51].

Research on the subject of postural control is still far from identifying a conclusive model of how balance is maintained in upright stance. Many sensory systems contribute to the regulation of posture, including vestibular, proprioceptive, and visual inputs. Moreover, these inputs may be integrated into the control scheme separately or in combination. Also, removing some of these systems can be difficult or invasive, requiring vibratory inputs, induction of ischemia, or anesthetization [65].

These factors make it difficult to evaluate the effects of any individual sensory system independently.

A possible scheme for the interaction of various systems contributing to postural control is illustrated in Figure 2–5. This highlights the ability of the central nervous system (CNS) to alter active stiffness directly, based on responses such as the muscle spindle. The CNS also integrates information from sensory pathways to alter the stiffness response at the ankle. Feed-forward pathways may also contribute to the alteration of ankle stiffness and body dynamics, including changes to postural sway.

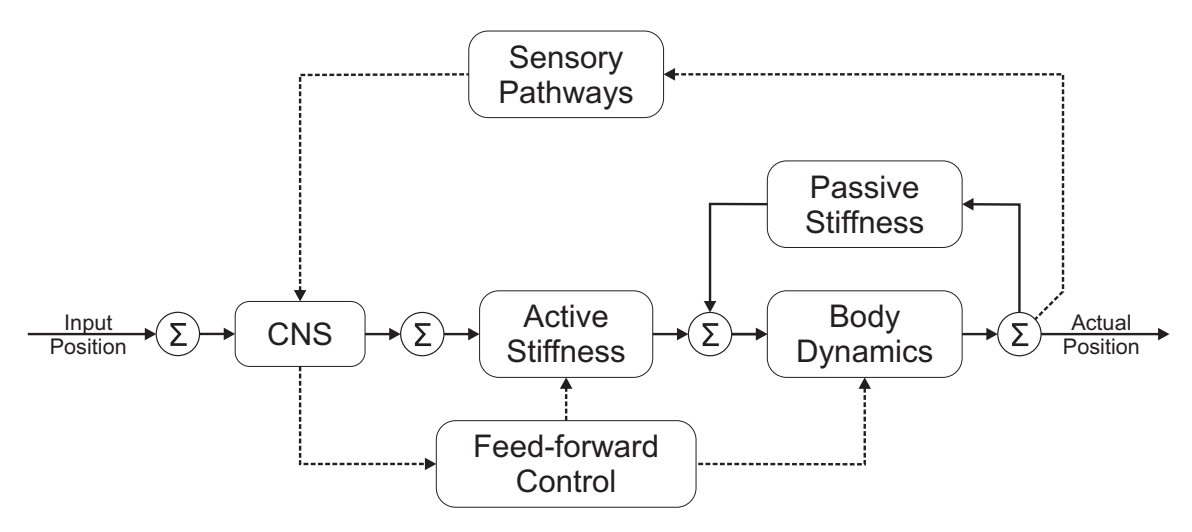


Figure 2–5: A general model of postural control. The CNS maintains postural stability by altering active muscle stiffness, based on sensory feedback. Some pathways may also generate torques by mechanisms which are not directly related to joint stiffness. The dotted lines represent connections whose models and contributions are uncertain.

There is no agreement in the literature regarding how these mechanisms contribute to postural control. Some groups assert that the passive intrinsic properties of the ankle muscles are sufficient to maintain posture, while others argue that active feedback or feedforward mechanisms are necessary. This section will provide an overview of the literature concerning these different contributors to upright standing.

2.3.1 Passive Control

The passive model of postural control is based on the assumption that humans can maintain balance without active intervention from the CNS. In other words, the CNS sets a constant level of muscle tone that is sufficient to stabilize the mass of the body during quiet stance. This condition would therefore result in a constant level of ankle stiffness. For the SIP mechanical model of posture, ankle stiffness would have to be greater than K_{crit} for the subject to remain upright.

This model of stance was proposed by Winter and colleagues, based on the results of studies of unperturbed quiet stance [71]. Using an optical tracking system with markers attached to key points on each subject, they estimated the position of the COM. COP data was measured using two force plates. The delay between the COP and COM movements was very short (less than 6ms), and they argued that this delay was too short to arise from active control mechanisms [71]. They later reported that ankle stiffness (estimated by regression of ankle torque and sway angle) was greater than K_{crit} , indicating that passive control was sufficient to maintain balance [74].

Some issues have been raised with this characterization of upright stance. Several studies have used a variety of techniques to study intrinsic stiffness during upright stance, ranging from perturbation of a visual scene, to simulation studies, to quiet stance on a perturbed support surface. Each reached the conclusion that intrinsic

stiffness alone is insufficient to stabilize posture. The passive stiffness values obtained from a variety of studies range from about 20-90% of K_{crit} [7, 31, 34, 45, 46, 52].

Loram et al. applied small perturbations with amplitudes similar to that of natural sway movements and estimated passive stiffness by fitting a second order model to the torque response. They found stiffness values averaging 91% of K_{crit} that remained constant despite changing muscle activation, suggesting that it was not a neurally controlled parameter [34]. This result necessitates some additional active modulation of ankle torque to compensate for the subcritical stiffness [34]. In a similar experiment, Kiemel et al. reported stiffness values of around 50% of K_{crit} using a frequency response approach [31].

Further evidence against the passive model of postural control came from the demonstration that the phase coordination of the COP and COM signals results from the physical laws governing upright stance. Morasso et al. simulated postural control using the dynamics of the SIP model assumed by Winter et al. Their simulations and analysis of the closed-loop transfer function of the SIP model showed that the COM acceleration was approximately proportional to the COM-COP difference. Additionally, their theoretical calculations resulted in the same in-phase relationship between COP and COM reported by Winter and colleagues [46]. While this supports the SIP as a model for postural dynamics, Morasso argued that the observed relationship between COP and COM was a necessity for the stability of the mechanical model, and could not be used to provide insight into the specific control mechanisms used by the subjects in Winter's experiments.

The ankle stiffness in the studies of Winter et al. was estimated simply by dividing the torque response by the size of the perturbation. This approach is flawed because it would include the effect of any tonic contraction in addition to the intrinsic stiffness [46]. Their calculation would require the demonstration that there is no neural modulation due to sway and that mechanical stretching is the sole cause of torque changes [34]. Since the Winter method relies on overall body dynamics, ankle stiffness calculated in this way will inevitably be larger than the critical value due to mechanical constraints, otherwise the subject would fall forward. Lastly, in order to consider this calculation of stiffness as valid, the system must operate under purely open-loop conditions and the viscous and inertial components can only contribute negligibly [45], both of which are inappropriate for the study of ankle stiffness [29].

While passive mechanisms play an important part in upright stance, they generate insufficient stiffness to maintain stability alone. Therefore, active mechanisms must be supplemental to the control of posture.

2.3.2 Active Control

The CNS can regulate balance and control stiffness in a multitude of ways. It can integrate information fed back from sensory pathways, including inputs from the visual, proprioceptive, and vestibular systems. The muscle spindle provides feedback to the CNS on the level and speed of muscle stretch, and can elicit a stabilizing reflex torque that can be modulated by the CNS. Additionally, feedforward pathways may be used by the CNS to react to anticipated changes in the position of the COM through a model of body dynamics. These control methods operate concurrently, however the relative contributions of each at any point in stance

are continuously changing. It is therefore difficult to isolate the contributions of each to overall postural control.

Joint Position and Velocity Feedback Mechanisms

Loram et al. suggested that sway may be controlled by an impulsive, ballistic process of muscle contraction [35]. By attaching an ultrasound scanner to the calf muscles, they measured changes the length of the soleus and gastrocnemius. They found that these muscles adjust their length about 2.8 times for each period in which the COM is moving in one direction, indicating subjects don't maintain stability with constant calf muscle activity. These length changes largely explained the control of the COM, keeping its velocity low while simultaneously being a source of its subsequent sway due to the inaccuracy of these contractions [35].

Feedback mechanisms are important for generating stabilizing torques based on reflex or sensory feedback. Nashner et al. recorded signals while applying rotational and translational perturbations. While some subjects did not use reflexes to augment ankle stiffness, some used long latency stretch reflexes in response to perturbations, augmenting the ankle stiffness in order to reduce postural sway. Subjects also altered their reflex gain over the course of subsequent experiments in which the usefulness of reflex responses was reduced; this was done by rotating the platform in reference to the postural sway, thus assisting the subject and reducing the necessity of reflexes. When the type of perturbation was suddenly changed, subjects adapted their reflex response to the new perturbations after a few additional trials [50].

Toft et al. studied the mechanical and EMG responses to stretch of the triceps surae muscles. At varying levels of background torque, they applied a rapid, 5° rotation about the ankle joint while collecting surface EMG signals from the soleus and gastrocnemius muscles. At low levels of voluntary contraction, the reflex component comprised two-thirds to one-third of the total force measured 200ms and 400ms after the perturbation. At higher levels of voluntary contraction, the reflex contribution to total force dropped to about ten percent [66].

Other studies have also shown that these short-latency reflexes do not contribute significantly to balance, citing their sensitivity to small inputs and absence during larger input perturbations [10]. However, there is potential for CNS modulation of the reflex stiffness when there is a change in the requirements of a given activity, even during simple activities like walking and standing [64]. This suggests that the influence of reflexes may be important in some situations and not in others [30].

Postural Feedback and Feed-forward Control

Masani et al. studied the role of velocity feedback as a contributor to anticipatory control of quiet stance. They observed an anticipatory modulation of the ankle extensor muscles with respect to the COM displacement and velocity. Lower leg electromyographic (EMG) activity preceded the body sway and was correlated with it [37]. This was in accordance with the idea that the maintenance of upright stance involves an anticipatory mechanism [12].

Gatev et al. also examined the correlation between COP and COM movements and muscle activity during quiet stance. They found that the phase of the lateral gastrocnemius muscle activity led that of the motion of the COM and COP. This contrasts with the idea of a simple servo-control mechanism for balance, in which muscles would activate in response to loading instead of activating before it occurs [15].

Later work by Masani et al. found that, while a feed-forward mechanism might exist, it was not a necessity; the anticipatory dynamics could be reproduced in simulation by a proportional-derivative (PD) controller. The COM velocity alone sufficed as an indicator of how the COM position would change and how the CNS should compensate for disturbances [37]. A PD controller was shown to be a workable solution for a wide array of control gains, feedback delays, and signal transduction delays [39].

Feed-forward neural pathways have been proposed as an explanation for anticipatory behavior. Fitzpatrick et al. applied small perturbations to subjects' waists and observed the effects on body sway and the soleus EMG [12]. They observed a loop gain for EMG modulation with position that was too low to maintain stability. This confirmed the importance of feedback mechanisms in the control of balance, but suggested that they were insufficient on their own. A feed-forward pathway was proposed since reflexes were smaller and insufficient in gain when unexpected disturbances occurred compared to when perturbations were expected [12].

Contralateral Dynamics

In quiet stance, the motions of the COP under each leg are different, although highly correlated to each other [75], and to the net COP location [72]. Studies that assume a SIP model consider the response of each leg as identical and, while this may be appropriate for studies of whole body motion, there is clear evidence that the inputs to one leg can alter the response in the other. To date, contralateral phenomena have been little-studied and their physiological basis and dynamic operation remain unclear.

Dietz et al. investigated the contralateral contribution to stance dynamics using a split-belt treadmill to apply different combinations of forward and backward accelerations. They observed a contralateral response whose dynamics depended on whether the two legs were perturbed in the same or different directions [9]. This establishes that, when modeling upright posture, contributions to stability from each leg cannot be considered identical.

A different study investigated the response to slip of the leading leg upon heel strike. Unwary subjects were exposed to a slippery floor surface. A strong correlation between the knee response in the slipping leg and that of the trailing leg was observed. Some of these context-dependent responses may have been passive, resulting from the dynamics of the fall, while others were ostensibly active strategies. The possibility of a continuum of contralateral responses that depends on the severity of slip and initial conditions was suggested, analogous to the hybrid utilization of ankle and hip strategies in upright stance [47].

The contralateral response is important since it completes the characterization of upright stance. The SIP model ignores any coordination between the response of each leg. A complete model of upright stance must account for passive, active, and contralateral mechanisms.

Sensorimotor Signal Contributions to Upright Stance

Voluntary contractions, reflex mechanisms, and other classes of involuntary responses contribute to the dynamic mechanical response of the ankle to disturbances or instabilities. However, studies have provided evidence that visual, vestibular and proprioceptive signals are incorporated in the control of stance. Information from each system can alter how the ankle responds to an input stimulus and change the current postural control strategy. While it is clear that these inputs affect stance, the conditions under which they contribute and their effect on balance control continue to be a point of focus of postural control research.

The influence of the senses can be tested by creating conflicts of information between the senses. One technique for testing the interaction of sensory signals is to place subjects within an environment in which the visual scene moves differently than indicated by the other senses. For instance, while the subject's feet may be firmly planted on the ground, the visual scene could be varied, indicating motion when none is occurring. Similarly, proprioceptive information could be reduced by rotating the support surface proportionally to body sway.

A linear combination of sensory cues is one possibility for the integration of sensory information into postural control. Visual information determines the orientation of the head, vestibular cues compare the head position to the gravity vector, and proprioceptors determine the orientation of the leg with respect to the support surface. One theory suggests that each system detects an error signal, and these error signals are summed linearly to generate a corrective torque [52]. In contrast, another

study asserts that somatosensory inputs are processed concurrently with vestibular signals. When perturbations were applied to both systems simultaneously, the responses changed in a manner that could not be explained by linear combination of sensory information [19]. Thus, the manner in which these inputs are processed requires further study.

Peterka et al. presented evidence for a phenomenon termed 'sensory reweighting', in which subjects make greater use of other senses when one sense provides unreliable information. Subjects were exposed to different combinations of visual and support surface perturbations. A sensory integration model, with the visual and postural perturbations as the inputs, was used to weight the contributions of each sense to the postural dynamics. As the amplitude of perturbations to either the visual scene or support surface increased, the associated gain decreased. This suggested reweighting was performed to reduce the instability created by the increasing amplitude of the perturbations [52]. In another experiment, when returning to a normal condition after a period during which the reliability of proprioceptive information was reduced, subjects became temporarily unstable and exhibited different body sway than during normal quiet stance. A feedback model of postural control allowing for sensory reweighting was able to predict this phenomenon. This suggested that subjects change the weights of sensory information in response to the current postural task and carry these weights temporarily to subsequent postural conditions [53].

Polastri et al. also examined sensory reweighting when applying sudden changes to both the visual input and perturbations applied to the base of support [54]. By suddenly changing the perturbations to each system, they found that subjects relied less on information received from the system that had been destabilized. Although their final results had large variance, their findings did display reciprocal modulation of visual and proprioceptive information. However, the pattern of reweighting differed depending the relative stability of proprioceptive information at the start of the experiment, indicating a possible nonlinear method of contribution from this input [54]. They suggested a more complicated situation than the linear sensorimotor fusion theory postulates, which merits more research on the topic.

Results from subjects with vestibulopathy support the idea of sensory reweighting and the linear combination of sensory inputs. Subjects with severe bilateral vestibular loss can control stance in a manner that is nearly normal, and in some cases completely indistinguishable from healthy subjects, using either visual or proprioceptive input [4]. However, when deprived of visual and proprioceptive information, they cannot maintain stability [49]. This contrasts with healthy subjects, who do not lose balance when deprived of these inputs [48]. Furthermore, while healthy subjects showed a decrease in gain with increasing stimulus amplitude, subjects with vestibulopathy did not, suggesting that they were incapable of sensory reweighting [52].

The effects of vision vary with balance strategy. For instance, Sarabon et al. examined the effect of removing vision on body sway when participants stood on a force platform in varying stances, ranging from parallel to single-leg standing. Eliminating vision had a significant effect on body sway in all stances. The interaction between vision on body sway also changed with changing stance types (i.e. - the

degree of change in body sway between eyes open and closed cases differed based on stance type). This suggests that sensory reweighting occurs when subjects adopt different stances. However, the physiological mechanism by which this occurs still remains unclear [57].

Ledin et al. changed the information received by proprioceptive inputs by fatiguing the triceps surae muscles or adding additional body weight. Subjects stood on a single force platform which was vibrated at a constant frequency of 85 Hz and performed eyes open and eyes closed trials. Postural sway increased with increasing muscle fatigue and additional body weight. Sway amplitude increased when vision was removed [32]. This agrees with observations from numerous other studies [12, 15, 35] and corroborates the link between changing postural dynamics and sensory information received by the CNS.

Subtle changes to sensory inputs may also change the stability and dynamics of balance. Fingertip contact with a rigid surface increases the amount of sensory information available, leading to a reduction in the amplitude of sway [26]. In an experiment by Jeka et al., subjects stood on a force platform with an inline foot configuration while placing the tip of their index finger on a touch plate which was perturbed at various frequencies in a direction parallel to the frontal plane. The frequency-domain relationship between the touch plate input and body sway information changed with varying touch plate perturbation frequency. This suggests that CNS strategy to control COM motion changes depending on the position and velocity information received from the somatosensory system [25]. It also highlights the importance of inputs from mechanoreceptors to the control of balance.

2.4 Joint Stiffness

Joint stiffness is the dynamic relation between the position of a joint and the torque acting about it, including both passive and active muscle torque generation mechanisms. Stiffness encompasses the complex mechanical behavior of the joint, characterizing its interaction with the environment, limb kinematics, the muscular mechanics that generate torques, and the articular mechanics [29]. Measuring joint stiffness makes it possible to separate the effects of active and passive contributions to joint torque.

Dynamic joint stiffness can be divided into two components: intrinsic and reflex stiffness. Intrinsic stiffness results from a combination of the passive viscoelastic properties of connective tissue and muscle, articular mechanics, and active muscle fibers [29]. Intrinsic stiffness is well-modeled using a second order, linear, underdamped system with elastic, viscous, and inertial parameters K, B, and I, respectively [30]. Reflex stiffness encompasses the torques generated from involuntary mechanisms including signals from the muscle spindle response to muscle stretch [29].

2.4.1 Modulation of Joint Stiffness

There is evidence that the nervous system can modulate intrinsic and reflex stiffness, as well the relative contribution of each to a postural task. These stiffness can be modulated as the requirements of the task change [64], and can also be modulated by changing the position of the joint or activation level of the ankle muscles. Furthermore, vestibular, visual, and proprioceptive inputs have been demonstrated to affect general postural dynamics, and these inputs may effect such changes by altering ankle stiffness directly. However, since most of the studies concerning sensory

input have not taken a system identification approach to ankle stiffness, we can't assert their specific influence on ankle dynamics.

Both intrinsic and reflex stiffness vary with joint position. For a constant level of tonic contraction, as the ankle moves toward the extremes of its range of motion, the intrinsic stiffness parameter 'K' increases [69]. Tested in a supine position, intrinsic stiffness also increases when the ankle is dorsiflexed [41, 70]. The magnitude of the reflex response also increases as the subject's ankle is moved toward dorsiflexion [41].

Various studies performed in the supine position have also shown that intrinsic stiffness varies with the activation level of the ankle muscles. This can result from contraction of the agonist muscles, leading to a change in net output torque, or co-contraction of the agonist-antagonist group, yielding no net change in output torque [36]. Subjects exhibit a minimum intrinsic stiffness value while at rest, which increases as the level of voluntary contraction is increased [6, 41, 68].

The level of background torque also has an effect of the reflex stiffness gain. Mirbagheri et al. discovered that the reflex torque increased significantly from the rest condition to the minimum voluntary contraction level, and decreased slightly thereafter [41]. In standing, muscle activity is variable with motion of the COM and COP. As the COM falls forward over the base of support, there is an increase in lateral gastrocnemius muscle activity. Conversely, as the COM moves backward, there is a decrease in lateral gastrocnemius activity [15]. As voluntary contraction affects stiffness, it is conceivable that contractions due to postural sway may also change ankle stiffness.

The CNS also has the ability to control intrinsic and reflex stiffness independently. When given real-time feedback of their elastic stiffness and reflex gain, subjects were able to modulate their reflex stiffness while keeping intrinsic stiffness constant [36].

The nature of the input to the ankle can additionally affect the reflex response. For an ankle experiment performed in a supine setting, as input amplitude increased, the reflex electromyographic (EMG) activity and torque increased in parallel [63]. In addition, high-frequency vibratory inputs tend to suppress the primary reflex response. This can be envisioned in task-dependent situations in which large reflex responses to small, repetitive inputs would cause an overreaction to the stimulus [63].

All of the studies of ankle stiffness modulation presented thus far were conducted with the subject lying supine. In comparison to upright stance, the roles of visual, proprioceptive and vestibular information are vastly different between the two cases. While the upright condition necessitates control of the an inverted pendulum, the supine position is inherently stable. Thus, it is conceivable that the modulation of intrinsic and reflex stiffness may differ between the two scenarios.

Bock et al. applied random pulses to subjects standing quietly on a bilateral hydraulic actuator. Reflex EMG increased and reflex torque decreased with increasing background torque (backward sway) [5], which is in agreement with another study that found that reflex torque increased as subjects swayed forward [9].

Experiments from our lab provided further evidence for the sway-dependent nature of postural control. Perturbations were applied bilaterally on a bilateral ankle actuator. System identification techniques were used to identify intrinsic and reflex stiffness components for several segments of data in which sway was observed to be relatively stationary. The intrinsic and reflex stiffness changed with ankle position. However, there was insufficient data to conclusively model the relationship of stiffness to position [3].

The dynamic response of the ankle is highly variable and depends on the state of the ankle joint, including its position and the activation level of its actuating muscles. Since joint position and activation level are constantly changing during upright stance, stiffness may also vary continuously. An ideal system identification technique would account for this constant variability; however, the construction of a method that satisfies this condition is non-trivial.

2.4.2 Measurement and Identification of Joint Stiffness

Measuring the intrinsic and reflex contributions to joint stiffness is important for understanding the source of a response and for relating it to physiology and postural control. Unfortunately, it is non-trivial to discern the source of a torque generated about a joint. This is because intrinsic and reflex torques appear and change together, making it difficult to distinguish one from the other [41]. Some studies have attempted to distinguish the two using surgical intervention or anesthesia. However, these methods are invasive, and it is difficult to establish the equivalence in the conditions between the normal and altered cases required for meaningful comparison [30]. Therefore, this document will focus primarily on analytical methods aimed at distinguishing the two torque components within a record.

System identification is the field concerned with identifying the dynamics of a system through the use of input and output data [28]. System identification methods

can be divided into parametric and non-parametric approaches. Parametric methods are useful for providing estimates of the system dynamics while using a minimal number of parameters. However, these methods require considerable a priori knowledge of the system structure and order.

Non-parametric methods are less efficient, but their success requires much less a priori information [28]. These methods can be divided into linear (or quasi-linear) and nonlinear categories. Linear techniques describe the joint dynamics by the identification of linear impulse response functions (IRFs), relating joint position to joint torque. This method provides an accurate picture of ankle dynamics under a limited range of conditions, when the operating point remains constant and reflex contributions to the output torque are minimal. However, this type of model does not function well when position or activation level change, a characteristic feature of upright stance [28, 29].

Nonlinear methods are more complex and better able to model the reflex dynamics of ankle joint stiffness [27, 28], which are modeled by a Hammerstein system. This consists of a static nonlinearity which precedes a linear system [28]. This model is used because responses relating half-wave rectified velocity to triceps surae reflex EMG signals accounted for more variance than purely linear [27] or quasi-linear models [30]. The parallel cascade technique incorporates these reflex dynamics into a method that simultaneously estimates the intrinsic and reflex contributions to total ankle stiffness.

It is important to note that a limitation of many postural control studies is that they do not take a system identification approach. Most studies focused on the patterns of sway or motion of the COP or COM, which provides information about whole body dynamics. Stiffness estimates are rarely presented, and therefore, the insight provided into joint dynamics is limited. A joint stiffness approach when studying the contribution of different senses would allow for a more thorough definition of the physiological background for the modeling of upright stance. These methods seek to separate the effects of active and passive mechanisms, whose contributions can become unclear when studying joint stiffness through whole body dynamics.

Parallel Cascade Identification Method

The parallel cascade model has been extensively used in our lab for the non-parametric identification of joint stiffness dynamics. The model structure is shown in Figure 2–6. The only measurable signals are input position and output net torque (the sum of intrinsic and reflex torques). This method analytically separates the two components from the input-output data.

The first step in the method involves a key assumption that permits the separation of the two responses. Kearney et al. noted that the conduction delay of a reflex is approximately 40 ms [28] while the intrinsic torque is an instantaneous mechanical response that lasts less than 40 ms after a rapid position perturbation [30]. The method therefore sets the length of the intrinsic IRF to 40ms to prevent reflex torques from influencing the estimate of the intrinsic dynamics [30]. The identification method is as follows:

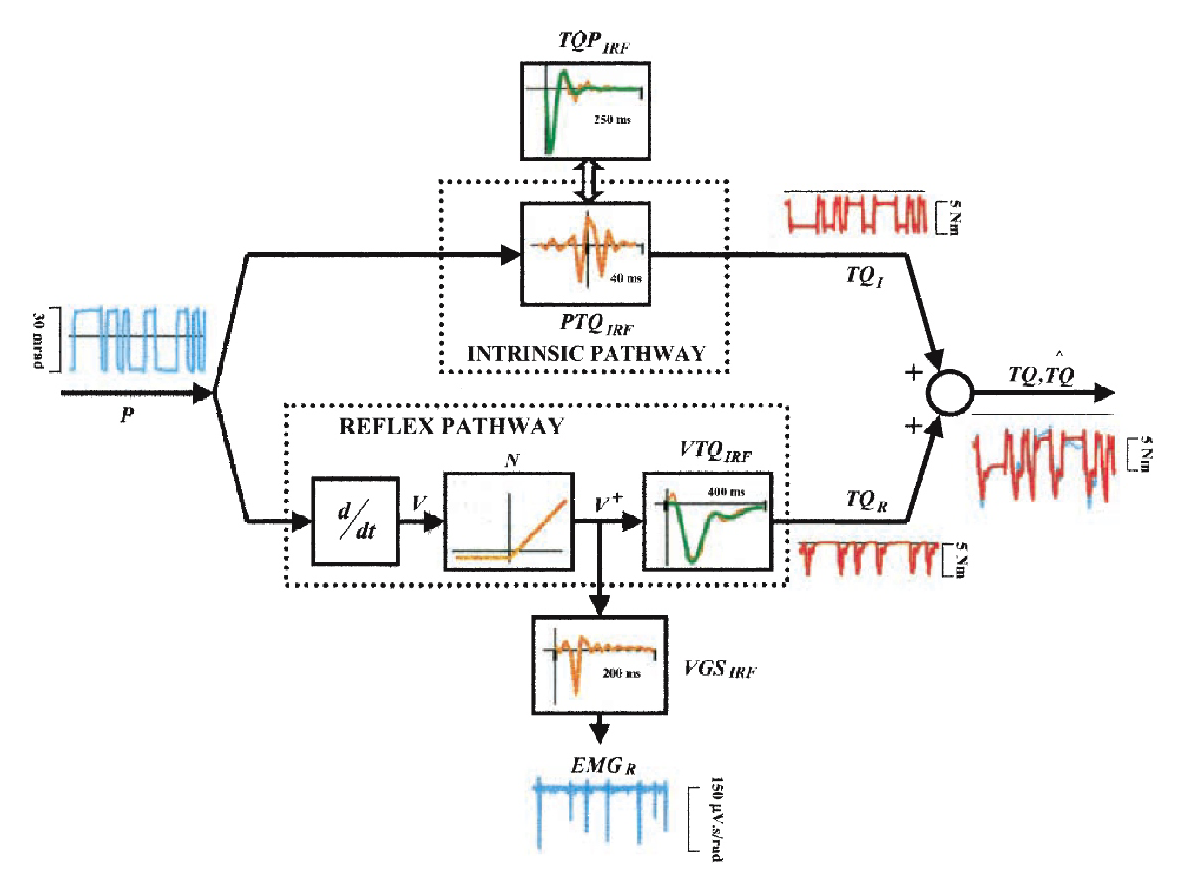


Figure 2–6: Parallel-cascade model of joint stiffness. Sample signals are shown in blue, modeled responses in red, non-parametric derived descriptions in orange and parametric fits to the non-parametric models in green. Intrinsic stiffness is estimated with a linear second order IRF in the upper pathway, while a Hammerstein system receiving velocity as an input models the reflex activity [41].

- 1. Intrinsic dynamics are first estimated by fitting a linear IRF to the torque. To avoid modeling the reflex dynamics, the length of the IRF is fixed to be less than 40 ms.
- 2. Using this estimate of the intrinsic pathway, an estimate of the intrinsic torque is generated by convolving the IRF with the input. This torque signal is then

subtracted from the output torque, leaving an estimate of the intrinsic residual torque.

- 3. The reflex system is identified using velocity as an input and the intrinsic residual torque as an output by a Hammerstein identification method. The model generated by this method is then used to generate an estimate of the reflex torque based on the velocity input.
- 4. Net output torque is predicted by summing the predicted intrinsic and reflex torques. The variance accounted for (VAF) is calculated at this stage.
- 5. The reflex residual torque is calculated by subtracting the estimated reflex torque from the output torque. The identification is then repeated from step 1, using the reflex residual torque as the output torque on which the intrinsic IRF is modeled. The procedure is repeated until there is no improvement in VAF.

This method produces non-parametric curves as estimates for the dynamics of the intrinsic and reflex components, which are difficult to interpret and compare between subjects and trials. Subsequently, parametric models may be fitted to these non-parametric curves to compare system parameters between subjects and trials.

It is possible to fit a parametric model to the intrinsic IRF generated by the parallel cascade method in order to extract the intrinsic stiffness parameters. This uses a linear least squares regression to model the second order linear dynamics. The transfer function takes the following form in the Laplace domain [30]:

$$\frac{\theta(s)}{TQ(s)} = \frac{1}{Is^2 + Bs + K} \tag{2.5}$$

In Equation 2.5, I, B, and K represent the intertial, viscous, and elastic parameters, respectively.

The reflex stiffness IRF can be parameterized using a second order low-pass system in series with a delay. Due to this delay, the corresponding samples are removed before the parametric fitting occurs. The form of the fitted equation is as follows [30]:

$$\frac{TQ_R(s)}{V(s)} = \frac{G}{(\frac{s}{\omega_0})^2 + 2\frac{\zeta}{\omega_0}s + 1}e^{-s\tau}$$
 (2.6)

In Equation 2.6, G symbolizes the gain of the reflex pathway, ω_0 the natural frequency, and ζ the damping ratio, and τ the delay. A more complex third order model is required to model the reflex dynamics in some cases. For example, fitting the third order model is necessary when contraction levels are high [42].

2.5 Rationale

Many of the aforementioned studies that directly measure the intrinsic and reflex stiffness have resulted from experiments in which the subject is supine or while balancing a simulated load. While these approaches are valuable, they are notably different from upright stance; the subject is inherently stable when lying down and does not bear the weight of their body. In other words, there is no requirement for the subject to maintain the stability of the inverted pendulum. The roles of proprioceptive and visual inputs are therefore different between these cases. Although asking a subject to stabilize a simulated load better mimics quiet stance, the subject

is typically seated or otherwise supported, causing similar changes to sensory contributions. Thus, the control of intrinsic and reflex mechanisms in upright stance is likely different than in other conditions.

The primary objective of this thesis is to investigate how ankle joint stiffness contributes to upright stance and to determine how this changes with the operating point. Prior studies have not addressed this fully and generally study overall postural dynamics, which give less insight into the torque-generating mechanisms used at the ankle. The material presented herein aims to investigate these time-varying properties of ankle joint stiffness in the setting of upright stance by identifying trends between measures of intrinsic/reflex stiffness and other parameters by which ankle stiffness may vary. The goals of this thesis will be as follows:

- 1. Estimate the intrinsic and reflex stiffness individually for a large collection of perturbation responses.
- 2. Examine the influence of postural sway on the estimated intrinsic and reflex stiffness.

CHAPTER 3 Experimental Methods

3.1 Experimental Apparatus

The evaluation of ankle joint stiffness requires the application of position perturbations to the ankle and the measurement of the torque produced in response. Experiments were carried out using a powerful hydraulic actuator and electronics that controlled the apparatus and sampled the signals. A computer system running MATLAB interfaced with the electronics and recorded actuator position, torque, and EMG signals from the muscles of the lower leg.

3.1.1 Bilateral Hydraulic Actuator

Posture will be treated as an open-loop system relating input position to output torque. While this is not always true in normal human stance, we can satisfy this condition in a few ways. We can use a maximally stiff interface which will not change position upon application of an external torque. In addition, by applying small perturbations, the ankle strategy will be predominantly in effect, thus minimizing torque contributions from other sources. To address these requirements, a hydraulic system was used to actuate each foot pedal of the apparatus.

The bilateral hydraulic actuator used in these experiments is shown in Figure 3–1. The subject stood on the foot plates with the axis of rotation of his/her ankle aligned to the axis of rotation of the actuator. A torque transducer was mounted between each foot plate and actuator to measure the torque generated about the

shaft. Mechanical stops and a hydraulic bypass were mounted on the shaft; each prohibits excessive rotation of the shaft. A potentiometer at the end of the shaft measured its rotation. The configuration was identical for each foot. Each component is explained in further detail in subsequent sections.

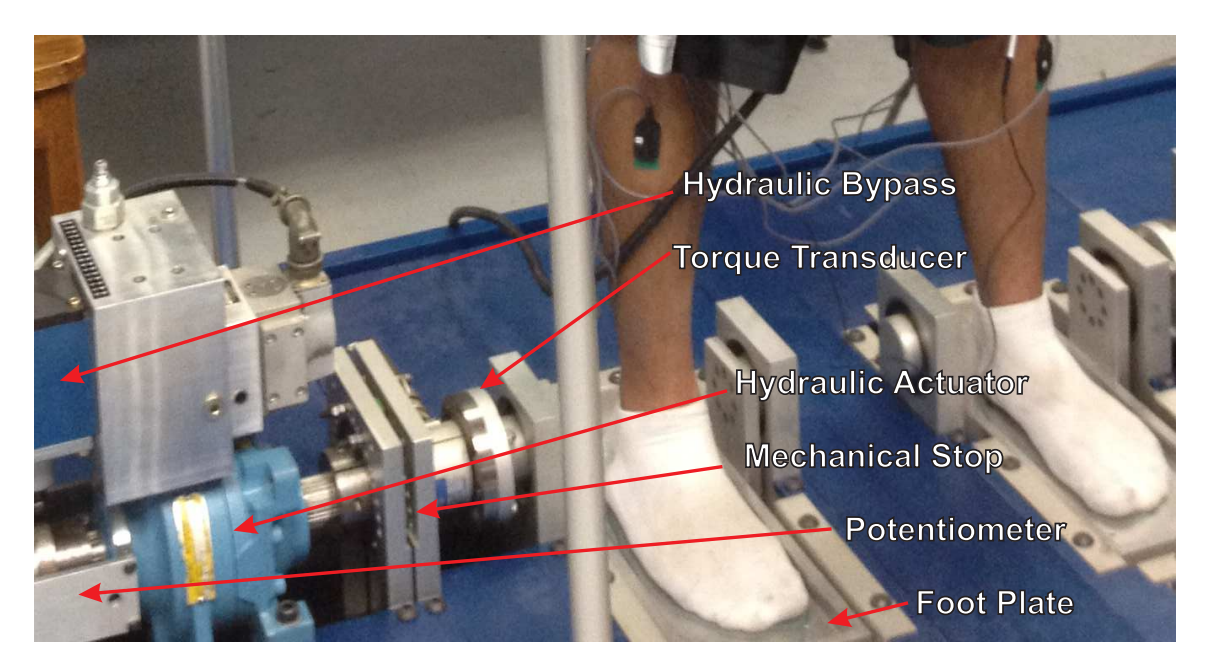


Figure 3–1: Bilateral hydraulic actuator with primary components labeled.

The rotary actuators (Rotac 26R-2 1V) could generate a maximum torque of 538 Nm [55] and has an operational bandwidth extending up to 20 Hz [13].

3.1.2 Safety Mechanisms

This hydraulic system was capable of applying large torques to the foot pedals, which could cause serious injury to the subject. In addition, subjects might lose their balance and fall during experimental trials. For these reasons, multiple safeguards were put in place to prevent subject injury [13, 55].

- Each actuator was equipped with a hydraulic bypass valve. Beyond ±20° of rotation, a cam attached to the actuator shaft would engage the plunger of the bypass system. This blocked hydraulic flow to the servo-valve, thus preventing rotation beyond a safe range of motion.
- 2. Steel bolts were mounted to a frame near both actuators to prevent the foot pedal from exceeding a safe range of motion. These act as mechanical stops and would engage the shaft to prevent rotation past $\pm 25^{\circ}$ from horizontal.
- 3. A panic button could be pressed at any time by the experimenter to cut off power to the hydraulic actuators.
- 4. Hydraulic power was automatically shut off if electrical power to the control system was interrupted.
- 5. Handrails were positioned on either side of the subject, who could grab hold of them at any time for stability.

3.1.3 Sensors

Potentiometer

The angular position of each foot pedal was measured by a potentiometer (Maurey Instruments 112-P19) attached to the shaft of each actuator. The potentiometers had a theoretical travel of up to $340^{\circ}\pm5^{\circ}$ with a linearity of 0.5%. The signals from the potentiometers were conditioned with custom-built conditioning modules calibrated to a sensitivity of $10\mathrm{V/rad}$. A positive angle indicated dorsiflexion whereas a negative angle indicated plantarflexion [55].

Torque Transducer

The torque produced by the subject on each foot pedal was measured by a Lebow 2100-5k torque transducer. The transducers were flanged reaction torque sensors with a capacity of 565 Nm and a torsional stiffness of 103941 Nm/rad (much greater than that of the ankle). The torque transducer signals were processed by custom strain gage conditioning modules to give an output of 20 Nm/V. As with the potentiometer, a positive torque signified dorsiflexion while a negative torque signified plantarflexion [55].

Load Cells

Each foot pedal was equipped with four stainless steel compression load cells (Omega LC302-100) located near each corner of the plate, as shown in Figure 3–2. The load cells were sandwiched between the foot pedal and a foot plate. Each load cell was connected to a strain gage conditioning module to give an output of 45 N/V; each had a maximum load capacity of 100 lb and measurement accuracy of 0.5%. With four load cell measurements from each pedal, the center of pressure for each foot and subject's weight could be measured [55].

With this load cell configuration, the center of pressure was calculated from the load on each foot pedal, as follows:

$$F_T = F_1 + F_2 + F_3 + F_4$$

$$COP_x(mm) = \frac{50F_1 - 50F_2 - 50F_3 + 50F_4}{F_T}$$

$$COP_y(mm) = \frac{145F_1 + 145F_2 - 145F_3 - 145F_4}{F_T}$$

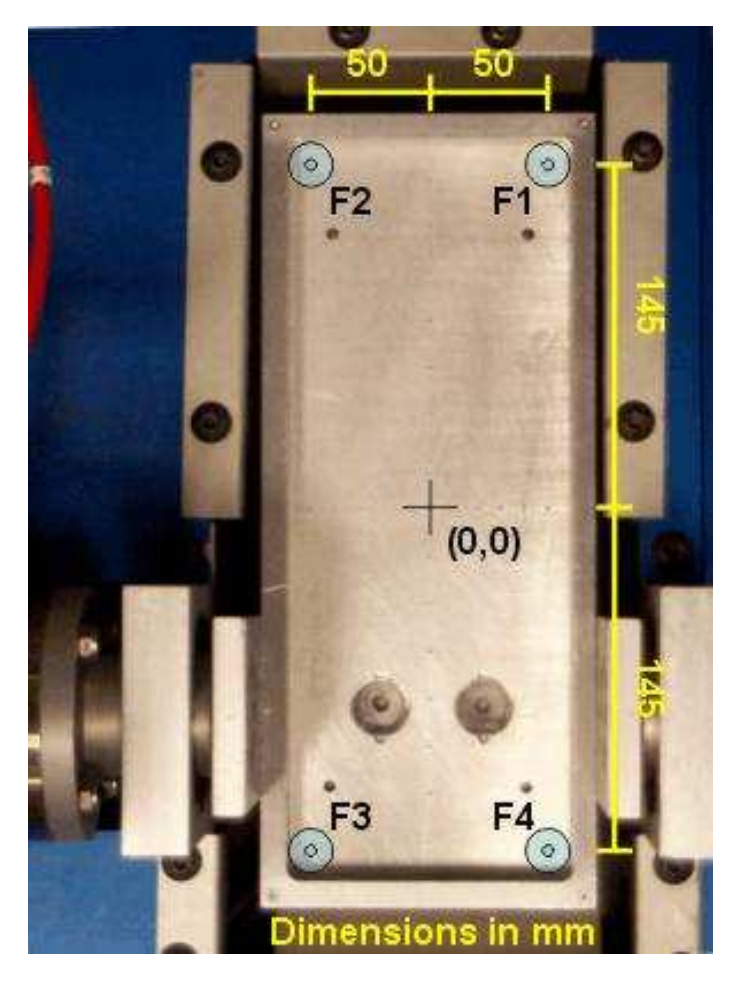


Figure 3–2: Foot pedal assembly with load cell positions indicated [55].

For accurate measurements, the load cell offsets must be removed from each sensor. These were measured and defined as the baseline reading when there was no subject on the horizontally oriented pedal.

Electromyography

The EMG sensors (Delsys Bagnoli DE-2.1) were single differential active electrodes with silver contacts spaced by 10cm, a resolution of $1.2\mu V$, and gain of 10. Each signal was measured with respect to a reference input lead. Electromyographic

activity was collected using an 8-channel EMG amplifier and interface unit, which further amplified the EMG signals by a gain of 100. This unit filters the EMG signals with a 20-2000 Hz pass band. The electrode power supply was electrically isolated from outlet power to prevent the risk of electric shock.

3.1.4 Data Acquisition and Experimental Control

A schematic of the system used to sample data and control the hydraulic actuator is shown in Figure 3–3. This involved communication between a host computer (SPASTIC) with a PCI expansion system (MAGMA) for data acquisition and a servo-control computer (RENSHAW) running the Matlab xPC environment (a real-time digital signal processing system).

MAGMA housed four 8-channel, 24-bit data acquisition cards (National Instruments DAQ 4472) capable of sampling a maximum of 32 signals at 1000Hz. A digital anti-aliasing filter with a 500Hz cut-off frequency was implemented within the card [13].

A proportional-derivative control model was developed in SIMULINK and compiled/loaded to RENSHAW through the use of two system-interface GUIs on SPAS-TIC. These GUIs were used to change the input signal and other parameters (e.g. -pedal offset, input gain, control gains), and to start or stop data collection.

RENSHAW was equipped with a 16-bit 8-channel analog to digital card (Computer Boards PCIM-DAS1602/16) and a 16-bit 6-channel digital to analog card (Computer Boards PCIM-DDA06/16). These allowed RENSHAW to acquire and control the actuator position and synchronize the signals with MAGMA. The actuator position signal was filtered with a constant delay low-pass anti-aliasing filter with

a cut-off frequency of 250Hz before being fed back to the controller. An Ethernet link was used to upload commands from SPASTIC to RENSHAW.

This data acquisition system was used to collect the signals shown in Table 3–1.

Table 3–1: Signals collected

Channel	Signal	Resolution
1	Left Angular Position	\pm 0.0087 rad
2	Right Angular Position	\pm 0.0087 rad
3	Left Torque	$\pm 0.04 \text{ Nm}$
4	Right Torque	$\pm 0.04 \text{ Nm}$
5-8	Left Pedal Load Cells	$\pm 0.01 \text{ N}$
9-12	Right Pedal Load Cells	$\pm 0.01 \text{ N}$
13	Left Lateral GS EMG	$\pm 1.2 \ \mu V$
14	Left Medial GS EMG	$\pm 1.2 \ \mu V$
15	Left Soleus EMG	$\pm 1.2 \ \mu V$
16	Left TA EMG	$\pm 1.2 \ \mu V$
17	Right Lateral GS EMG	$\pm 1.2 \ \mu V$
18	Right Medial GS EMG	$\pm 1.2 \ \mu V$
19	Right Soleus EMG	$\pm 1.2 \ \mu V$
20	Right TA EMG	$\pm 1.2 \ \mu V$

3.2 Experimental Paradigms

Nine subjects were examined: they ranged from 23 to 29 years of age with no history of serious leg injuries, neuromuscular disease, or other conditions that might interfere with normal balance. Subject characteristics are shown in Table 3–2.

3.2.1 Subject Preparation

EMG electrodes were attached to the TA and TS muscles. The lateral GS electrode was placed approximately 1/3 of the distance between the head of the fibula and heel, on the belly of the lateral GS muscle. A similar approach was used for the medial GS head, however the electrode was placed slightly lower to position

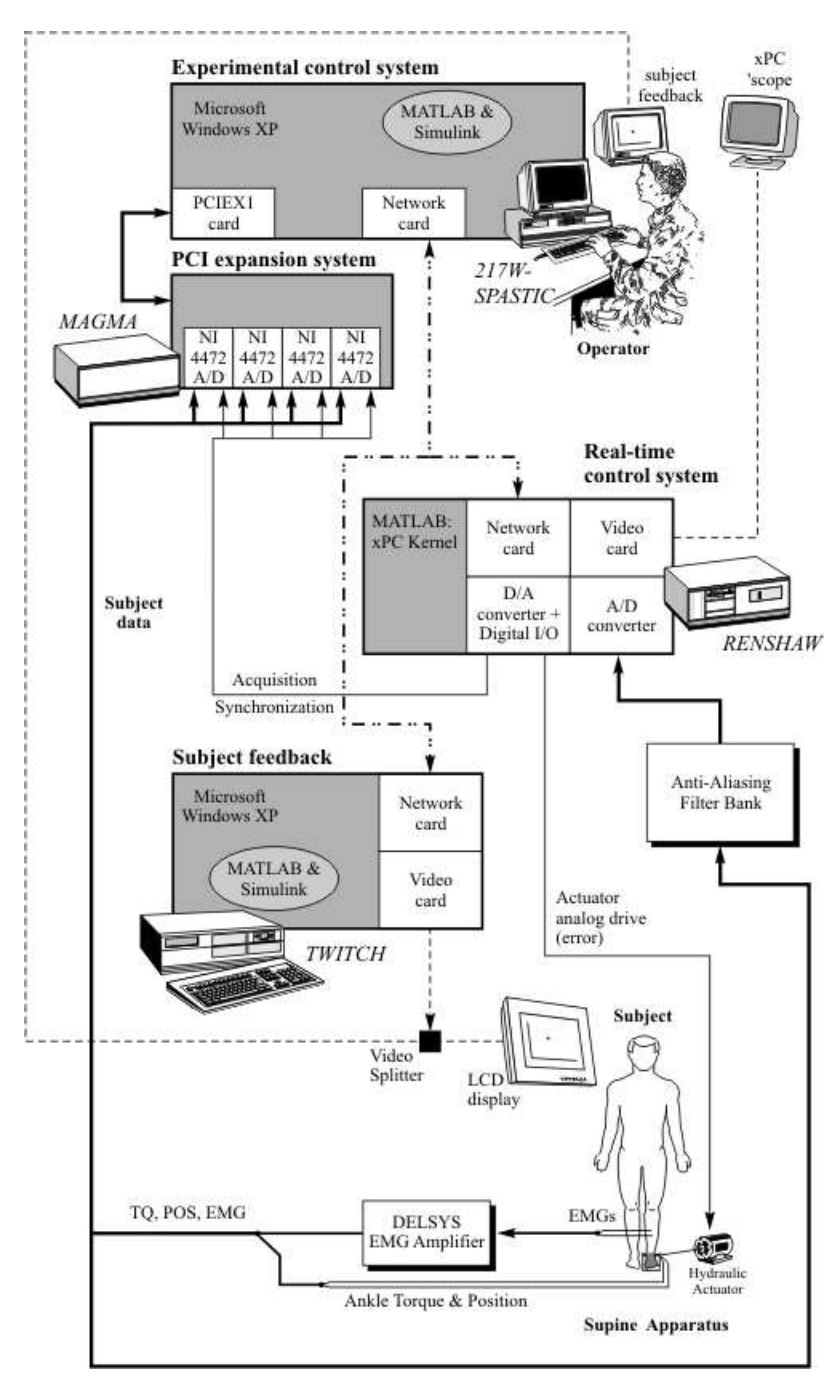


Figure 3–3: Diagram of the electronics setup for experimental data acquisition [55].

Table 3–2: Gender, age, height, and weight for each subject.

Subject	Gender	Age	Height (cm)	Weight (kg)
1	Female	27	162	76.2
2	Female	24	173	72.6
3	Male	24	182	64.2
4	Male	24	171	80.0
5	Female	23	170	60.8
6	Male	25	183	79.4
7	Male	25	188	70.4
8	Male	29	170	54.3
9	Male	26	168	77.8

it on the muscle belly. The TA electrode was placed on the belly of the TA at a similar height to the lateral GS EMG. The soleus electrode was placed on the center of the leg approximately halfway between the heel and lower edge of the medial GS.

Before placing electrodes on the skin, subjects were asked to shave small patches of skin corresponding to the electrode placement locations. These locations were then wiped with alcohol swabs to remove any dead skin or oils that could impede EMG signal acquisition. Each EMG electrode was oriented parallel to the muscle fiber and attached to the skin using double-sided adhesive tape. The reference electrode was affixed to the left patella. The quality of each EMG connection was observed and verified using an oscilloscope. During this verification, the subject was asked to stand on their toes to test the signals from both GS muscles and soleus muscles. Subjects were then instructed to lift their toes to test the TA EMG signal. The EMG cables were attached to the subject's clothing and again to the handrails in order to minimize cable movement artifacts.

Subsequently, the axis of rotation of the ankle (axis of the talocrural joint, see 3–4) was aligned with that of the actuator. The measurements used to locate the axis of rotation for the ankle of each subject were based on average data collected from the cadaveric study of human ankle anthropometry [22]. After aligning the subject and the actuator, the outline of the foot was traced on each foot pedal to facilitate repositioning between trials, in case the subject required to stretch/rest/etc.

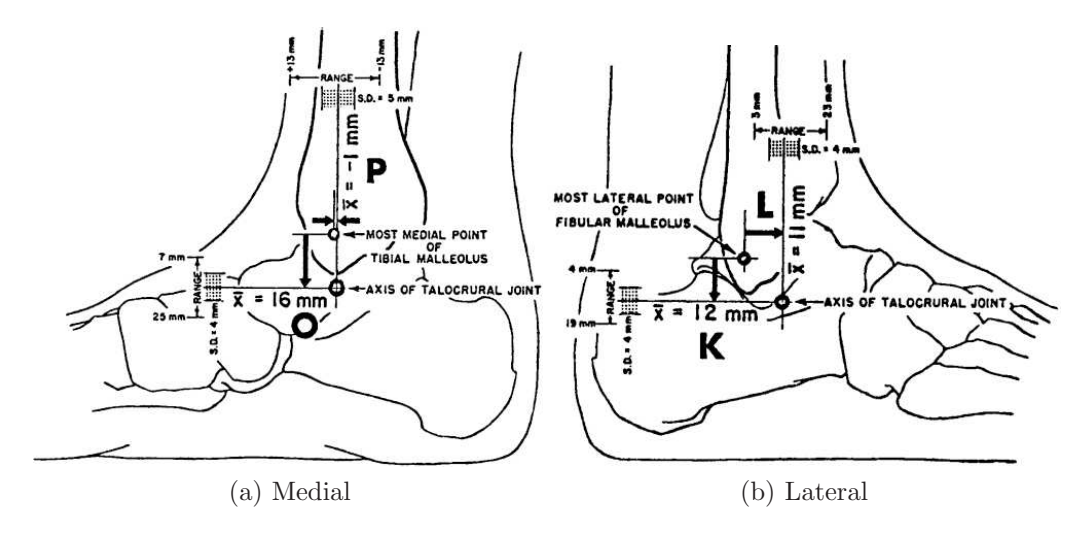


Figure 3–4: Axis of rotation of the talocrural joint as measured from ankle anatomical landmarks [22].

3.2.2 Trial Types and Execution

Data were acquired for 120 seconds for each trial, and a total of ten perturbed trials were performed with each subject. This number of trials was decided upon as an acceptable trade-off between the amount of data collected and total experiment length after preliminary analysis of pilot data. The trial types are as follows:

• Bias Acquisition: Data were acquired for 10 seconds with the pedals positioned horizontally, with no perturbations applied, and without a subject on

the actuator. This was performed to measure the offsets of the torque sensors and load cells.

- Quiet Stance: The pedals were positioned horizontally and no perturbations were applied. The subject stood relaxed with arms at their sides, looking straight ahead at a target positioned at eye-level on the wall. This trial was used for reference when comparing background torque patterns between trials and subjects.
- Bilateral Perturbed Normal Stance: Subjects were instructed to stand relaxed and look straight ahead while PRBS perturbations were applied to both foot pedals simultaneously.
- Bilateral Perturbed Forward Leaning: For this subset of experiments, subjects were instructed to lean slightly forward for the duration of the trial. This was done to offset the mean torque level for the trial. Subject were instructed to lean slightly forward and maintain their balance slightly more on the balls of their feet than they would during normal stance. No torque feedback was provided, since this could potentially have altered the subject's control strategy. Subjects were allowed to acclimate themselves to the perturbations in conjunction with the leaning to ensure that they could maintain stability throughout the trial and to reduce any associated discomfort.
- Bilateral Perturbed Backward Leaning: For this subset of experiments, subjects were instructed to lean slightly backward to offset the mean torque level for the trial. The subject was instructed to maintain their balance slightly

more on the heels of their feet than normal. Otherwise, this trial was conducted identically to the forward leaning trial.

Experiments consisted of a total of twelve trials. The bias acquisition and quiet stance trials were conducted first. Afterward, the order of the trials was as follows: normal(x2), forward lean, backward lean, normal(x2), forward lean, backward lean, normal(x2). This order was chosen to reduce fatigue that could potentially have been caused by conducting multiple consecutive leaning trials, as they require increased background activation of the lower leg muscles. This order was also chosen to allow investigation of the effects of leaning trials on subsequent normal trials. However, no such effects were observed.

3.2.3 Input Signal

For trials in which perturbations were applied, the signal used was a pseudorandom binary input (PRBS) with a peak-to-peak amplitude of 0.03 radians and a minimum switching time of 500ms (see Figure 3–5). The input signals for each foot were generated independently and were uncorrelated, as shown in Figure 3–6. Perturbations were switched on 10 seconds or more before the onset of data recording in order to eliminate any transient effects, since subjects require a few seconds to adapt a consistent control strategy after an unexpected change in the motion of the support surface [50].

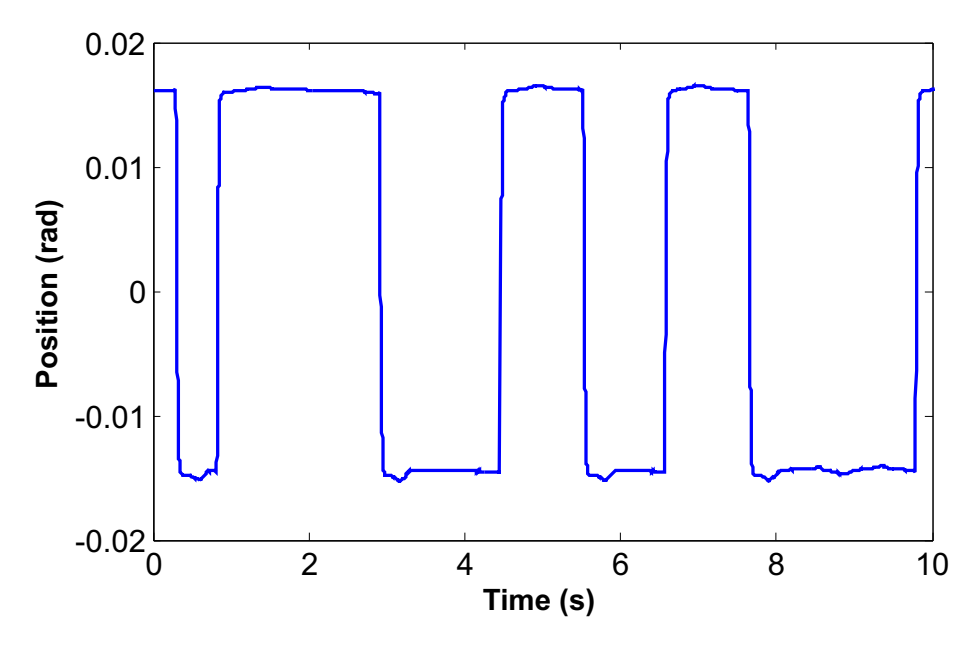


Figure 3–5: Ten seconds of a typical PRBS signal recorded from the potentiometer.

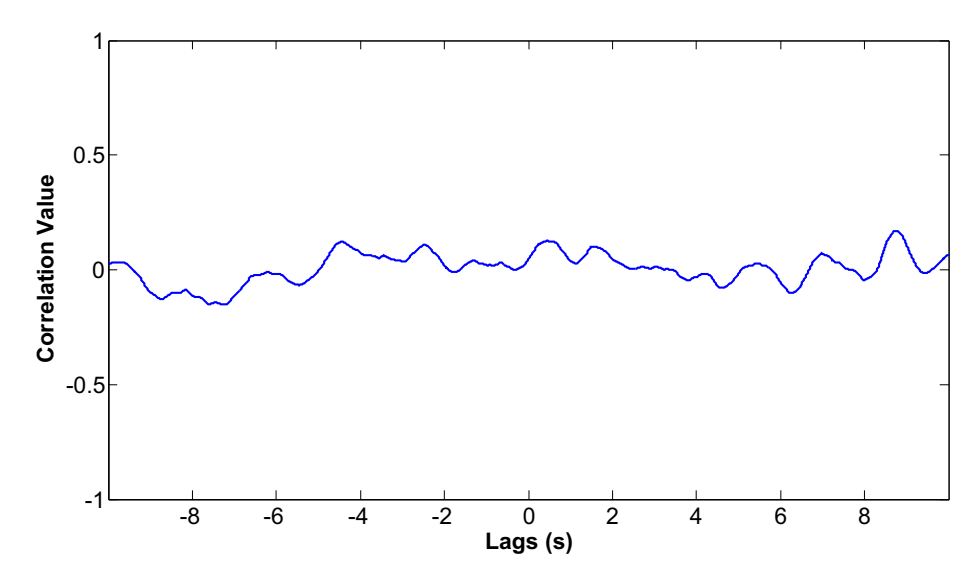


Figure 3–6: Cross-correlation between left and right input PRBS signals for a typical trial.

CHAPTER 4 System Identification Methods and Non-Results

This chapter outlines the initial attempts at identifying joint stiffness as postural sway changed using the parallel cascade method. The method was first applied to full records of data and subsequently to short segments. Ultimately, the parallel cascade method was inadequate for modeling the non-stationary nature of upright stance, due to the phenomenon of postural sway.

For the experiments presented in this chapter, the input signal used was a PRBS signal with a 0.03 radian peak-peak amplitude and switching rate of 200ms. All experiments were performed during perturbed quiet stance.

4.1 Parallel Cascade Identification - Full Record

4.1.1 Methods

In this section, data from a previously recorded supine experiment are included. In this case, the subject lay supine with his ankle attached to the actuator while rapid pseudo-random arbitrary level (PRALDS) perturbations were applied about the neutral position at the resting state.

Initial attempts to identify intrinsic and reflex stiffness at the ankle during upright experiments were performed on two minute long data records. Position perturbations were applied bilaterally to the actuator foot pedals while the subject stood quietly. Data were sampled at 1 kHz and then decimated to 200 Hz for analysis, and the parallel cascade identification was applied. After discovering issues with this

approach, sway torque was estimated by low-pass filtering the raw torque with a 1 Hz cut-off frequency and 60dB attenuation at 3 Hz. However, as will be explained in Section 4.1.2, issues with the low-pass filter estimation of sway torque prevented a successful parallel cascade identification.

4.1.2 Results

Several issues were discovered when applying this approach to upright standing. As subjects maintained posture, they swayed back and forth, as described in the literature review. Sway torque cannot be reliably predicted, but it is nevertheless present in the torque recorded from the actuator. Since the parallel cascade method does not account for sway torque, this signal effectively acted as a large noise source.

Parallel Cascade Identification

A typical parallel-cascade identification is shown in Figure 4–1 for both the supine and upright stance cases. While there was some dynamic activity remaining in the residuals of the supine case, the parallel cascade method achieved a 92% VAF. By contrast, the identification on the upright stance case was significantly less accurate, achieving only a 44% VAF. The residuals for upright stance showed significant and high-amplitude low-frequency variation, which was also displayed in the power spectrum in Figure 4–2. This could be attributed to postural sway torque, as the same phenomenon is not observed in the supine case. Thus, to improve the estimates produced by the parallel cascade method, it was necessary to remove this low-frequency torque signal.

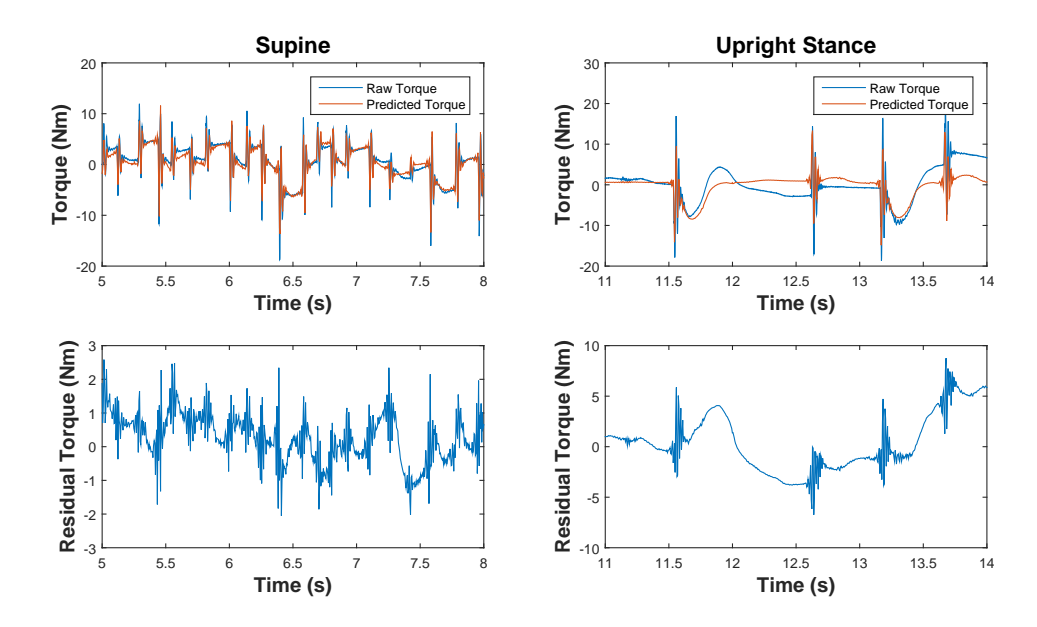


Figure 4–1: Sample fit for the parallel cascade method used on a supine experimental data (left) and upright stance experimental data (right), with residuals shown in the lower panels. The supine fitting achieved a 92% VAF while the upright stance fitting yielded a 44% VAF.

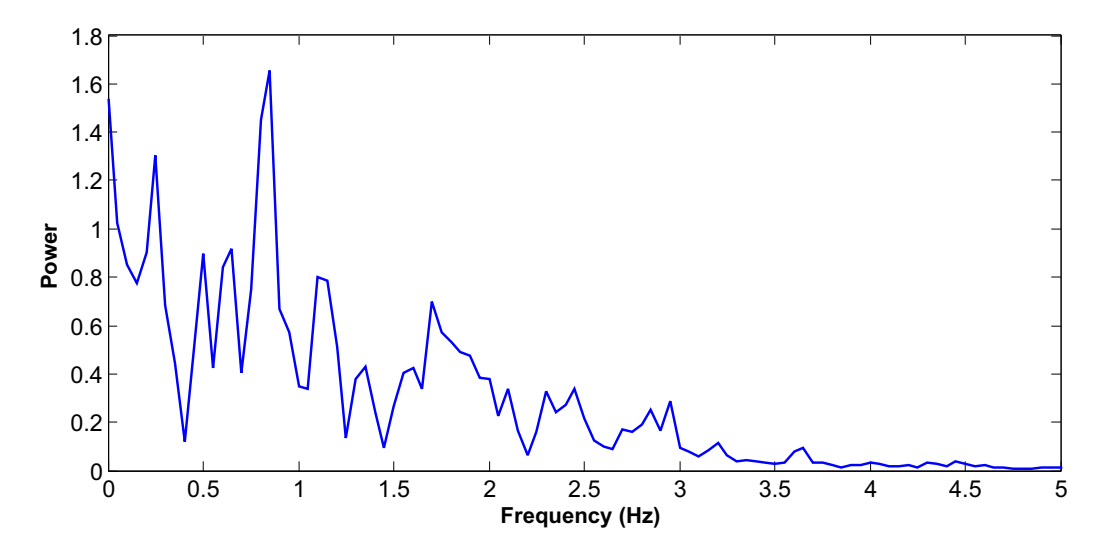


Figure 4–2: Power spectrum of the residuals from a parallel cascade fitting.

Calculating Sway Torque for Unperturbed Experiments

Figure 4–3 shows the power of the raw torque signal from both quiet and perturbed experiments. The top panel (quiet stance) indicates that much of the power in sway torque is below approximately 0.2 Hz. While it would seem that applying filters with a break frequency of about 0.2 Hz be ideal, sway torque had important content at frequencies higher than 0.2 Hz, which will be shown later. The frequency content changed when perturbations were applied, though ideally the filtering would not remove any important content from the signal. Low-pass filters with break frequencies ranging from 0.2 Hz to 2 Hz were applied in the attempt to remove only the sway torque. These filters were constructed using MATLAB's filter design tool, which was set to produce equiripple filters with a 60dB attenuation before 5 Hz.

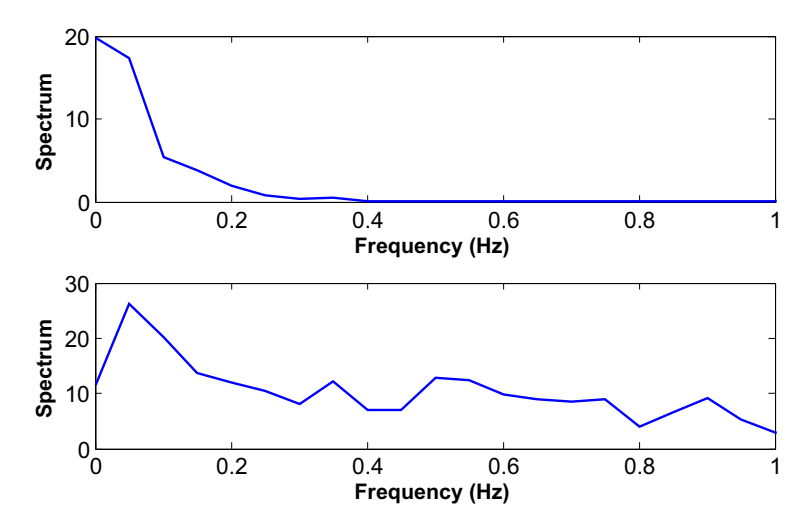


Figure 4–3: Low-frequency power for torque from a sample quiet stance experiment (top) and bilateral experiment (bottom). The reflexes generated in an experiment add low-frequency power to the spectrum.

Figure 4–4 shows a sample filtering of a torque record from a quiet stance experiment. A 0.5 Hz filter was incapable of fully capturing the torque; it underestimated

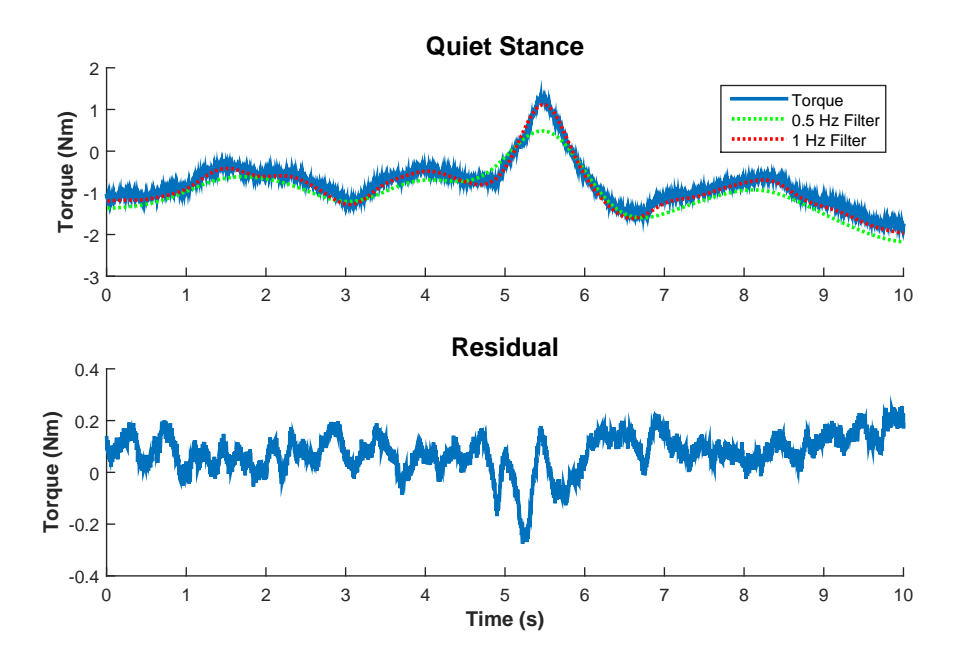


Figure 4–4: Sample calculations of sway torque collected from experiments without perturbations. The residuals shown are for the 1 Hz filter.

the peak at 5.5s and displayed a consistent negative bias throughout most of the rest of the window. The 1 Hz filter was much better at capturing the torque dynamics of quiet stance. While the filtering is less accurate around the peak at 5.5 seconds, on average, it fits the torque well, yielding a VAF of 99.2%.

Calculating Sway Torque for Perturbed Experiments

The task of removing sway torque became more difficult when perturbations were applied. Perturbations induced intrinsic and reflex responses, both of which would ideally be left unaffected by the filtering process. Unfortunately, filtering the perturbed torque similarly to the quiet stance experiments was inadequate. Figure 4–5 shows the 1 Hz filter applied to perturbed supine and upright experiments. The supine resting condition experiment is shown as a benchmark, since in this

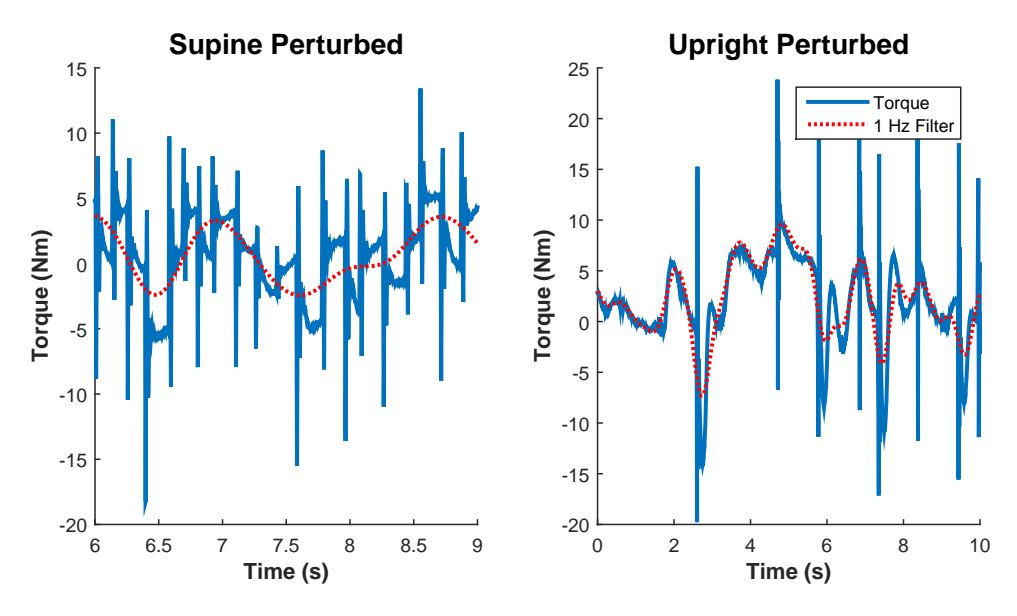


Figure 4–5: Sample calculations of sway torque for experiments performed in the resting supine condition (left) and in upright stance (right).

scenario, the subject was lying flat with his/her ankle strapped into an actuator. In this case, we did not expect any sway torque, considering that the ankle was not required to balance the load of the body. However, when filtering the torque similarly to the quiet stance case, we obtained a non-zero signal. This shows that the addition of perturbations causes the filter to capture dynamics additional to the sway torque alone. It is also evident in the upright perturbed case that just prior to the perturbations, when there was no reflex or intrinsic activity, the filtered signal tended not to match the torque. Furthermore, for dorsiflexing perturbations eliciting reflexes, the filtered signal reached a minimum at the same point as the peak of the reflex response. This suggested that the filtered signal is affected by the reflex response.

Summary

All subjects exhibited changing postural sway torque throughout the course of upright stance experiments. This signal degraded the estimation of the parallel cascade method; removing sway torque would be integral to the method's functioning in upright stance. However, estimating sway torque became non-trivial once perturbations were applied. Simple low-pass filtering methods that functioned in the quiet stance case were not accurate in the presence of perturbations. Furthermore, while there is evidence that intrinsic and reflex stiffness change with postural sway, the parallel cascade method is unable to identify time-varying dynamics. If stiffness was indeed changing throughout the course of an experiment, additional errors would be present in the identification. Therefore, the parallel cascade method was subsequently applied to segments of data which were relatively stationary in background torque. By doing this, sway torque would not need to be removed and joint stiffness would be assumed to be constant within these segments.

4.2 Parallel Cascade Identification - Short Segments

4.2.1 Methods

Although subjects exhibit varying postural sway over the course of an experiment, it was hypothesized that segments of data existed that would be quasi-stationary in sway torque and stiffness. The time-invariant parallel cascade method could then be used with these shorter, quasi-stationary segments to circumvent the issues encountered in the previous section, since sway torque would need not be subtracted. This would allow for the identification of intrinsic and reflex stiffness for subdivisions of the full experimental record, each subdivision having a different level

of sway torque. Using multiple subdivisions, a relationship between sway torque and stiffness could be reached.

Short segments were identified from the full torque record based on the properties of the estimated sway torque (raw torque filtered by a 1 Hz low-pass filter). By visually examining the torque from a full experiment, the most stationary periods were first chosen based on their variability compared to neighboring sections. A number of these sections were then classified by a moving window calculations of the mean and standard deviation. Stationary segments were defined as those in which these measures matched the visually determined segments. Any segment less than 10 seconds long that was identified as stationary was discarded, since the parallel cascade fails for very short data records. Sample segments are shown in Figure 4–6.

4.2.2 Results

This approach encountered several difficulties, mostly due to the nature of upright stance. Firstly, few stationary periods existed within each experimental record. For a two-minute experiment, typically fewer than three segments were found. This would cause issues in the practicality of gathering enough stationary segments to establish trends between stiffness and background torque. Secondly, the segments which were found were typically very short in duration (generally less than 15 seconds, see Figure 4–6). This was problematic for the parallel cascade method, since its performance improves with longer data records. Furthermore, even within the assumed-stationary periods, sway torque was still present and the background EMG activation was also highly variable. Lastly, a slight change in the data window used for identification could cause a drastically different result in the fit quality and the

identified Hammerstein system. This suggests that these periods were not truly stationary.

In most stationary segments, the parallel cascade identification achieved a VAF similar to the fit on the whole record. Figure 4–7 shows a 12 second parallel cascade fit on the stationary window from 8-20 seconds shown in Figure 4–6, which achieved a VAF of 85%. The residuals show that, even in a segment that was presumed to be stationary in sway torque, there is still a low-frequency trend that is not modeled.

The Hammerstein system from this parallel cascade identification is shown in Figure 4–8, which would suggest that reflexes are a linear phenomenon. However, considering the previous research on ankle reflexes, this conclusion is incorrect. This observation may have occurred because the reflex pathway modeled some of the sway torque that occurred in this window. The disappearance of the expected 40ms delay in the reflex IRF also supports this possibility. These observations were consistent among several different short segments of data and between a few subjects. Thus, as a whole, the results from using the parallel cascade method on short segments of data cannot be trusted to give reliable estimates of stiffness dynamics.

4.3 Conclusion

In these experiments of ankle joint stiffness, no conditions were found under which the parallel cascade identification would produce reliable results. While the removal of the non-stationary sway torque was necessary for proper identification using the parallel cascade method, it was non-trivial. Circumventing this issue using short segments of pseudo-stationary data proved fruitless also, as the sway torque

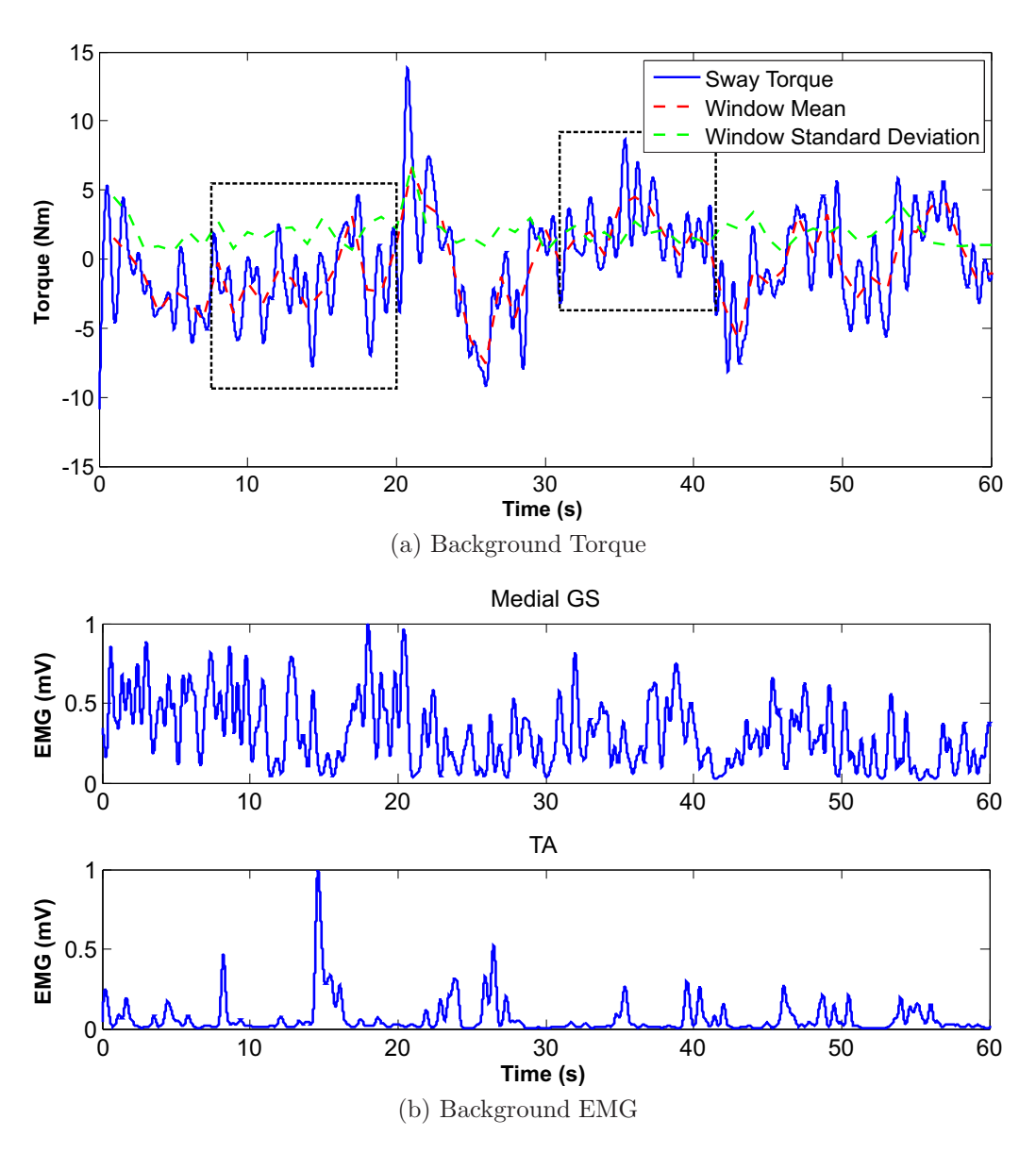


Figure 4–6: Sample background torque (sway torque) with segments and background EMG (raw EMG signal low-pass filtered at 1 Hz with reflex EMG removed) for a bilaterally perturbed experiment.

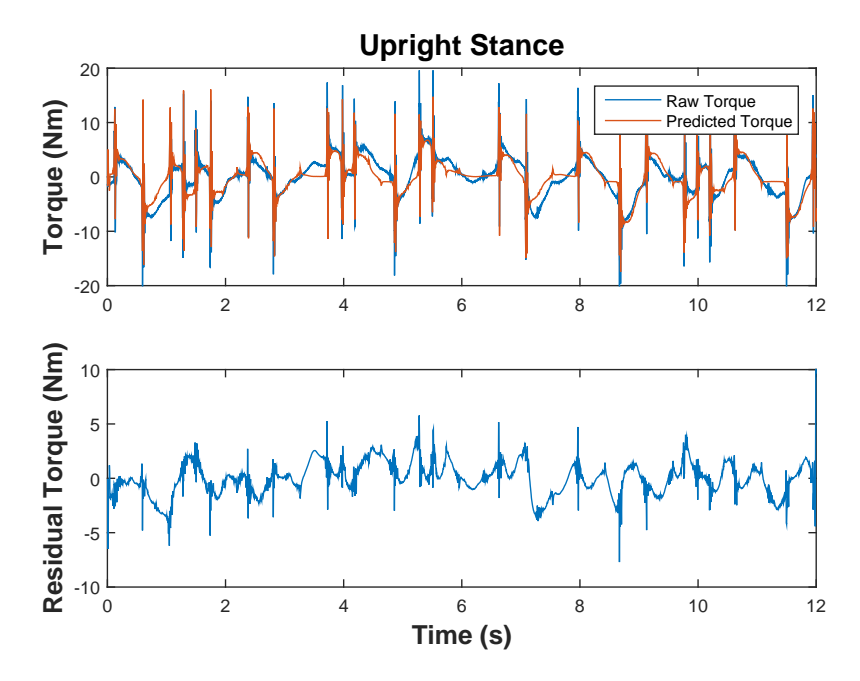


Figure 4–7: Parallel cascade identification performed on 12 seconds of experimental data. This example achieved a VAF of 85%.

was never truly stationary. The non-stationarity led to drastic changes in the identification results for small changes in the window size or position. The method would furthermore have been impractical for creating trends between sway torque and stiffness. Therefore, it was decided to observe the responses to individual position perturbations and determine the covariation of the intrinsic and reflex stiffness with background torque and muscle activity.

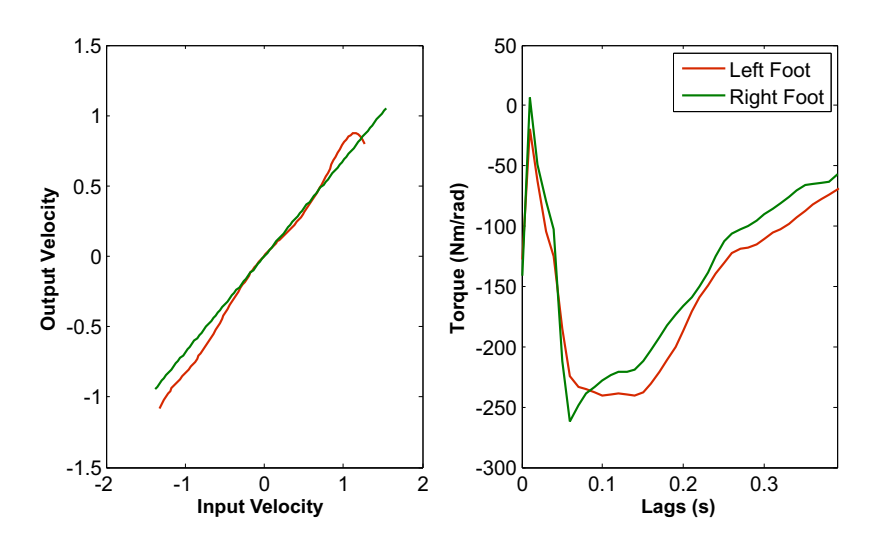


Figure 4–8: Identified Hammerstein system for the previously shown segment of data.

CHAPTER 5 Individual Response Processing and Analysis

System identification techniques were the first methods employed to identify the modulation of ankle joint stiffness. These methods unfortunately proved unable to capture the dynamics of joint stiffness during upright stance. A simpler method was then employed, in which the intrinsic and reflex magnitudes were calculated for each perturbation response. The background torque was evaluated for each response and compared with the intrinsic and reflex parameters. This chapter describes the methods used determine these parameters and the trends observed between them.

5.1 Methods

Each experiment or set of data was first divided into a collection of individual responses. A spike-detection method was applied to the pedal velocity signal (the derivative of the potentiometer signal) to identify the timing of the responses. Peak velocity occurred very near to the onset of each perturbation and its position was reliable between perturbations, which made it ideal for this purpose. The threshold for spike detection was determined by visual inspection of the velocity data and was set to 25% of the maximum or minimum value of the pedal velocity, depending on the direction of the perturbation. Sample spike detections are shown in Figure 5–1.

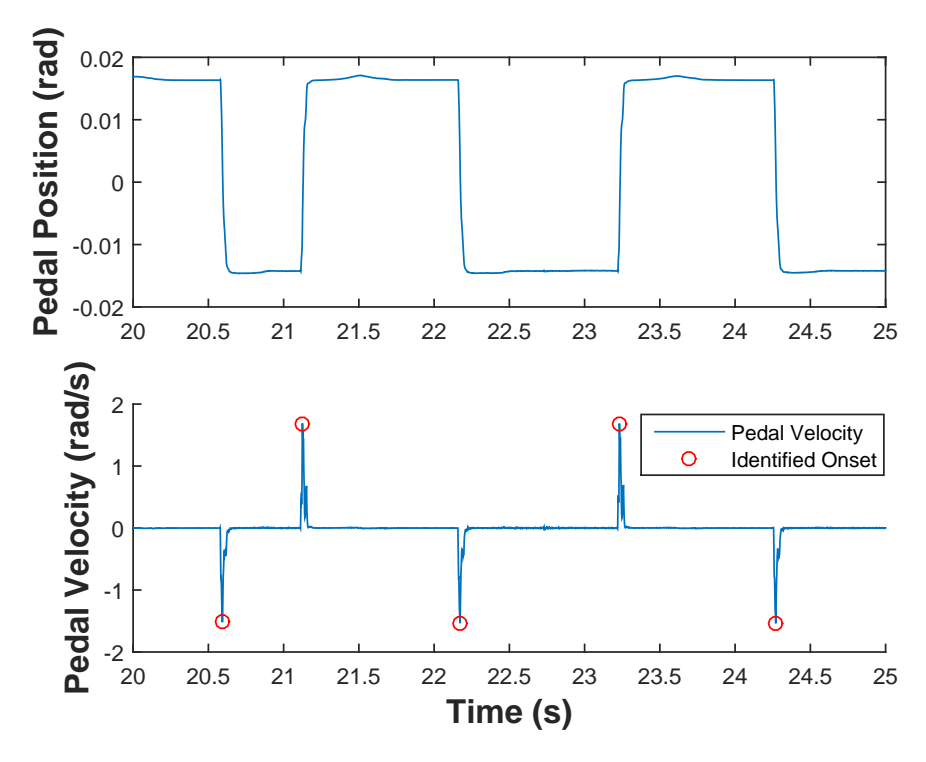


Figure 5–1: Sample spike detections for pedal velocity. Pedal position is normalized between -1 and 1. The onsets shown are the time values identified by the spike detection algorithm.

A response was defined as the period from 50ms before peak velocity to 450ms after. To facilitate parameterization, each response was subdivided into four subsections: pre-response, intrinsic response, reflex response, and post-reflex. Figure 5–2 shows these subdivisions for a typical response.

The lengths of these subsections were chosen following visual inspection of many responses from multiple subjects. Typically, the intrinsic response began around 40ms after the beginning of the window (or 10ms prior to peak velocity). The reflex torque began shortly after the intrinsic response, at approximately 90ms. Since the intrinsic response had not subsided completely by this time in the window, the start

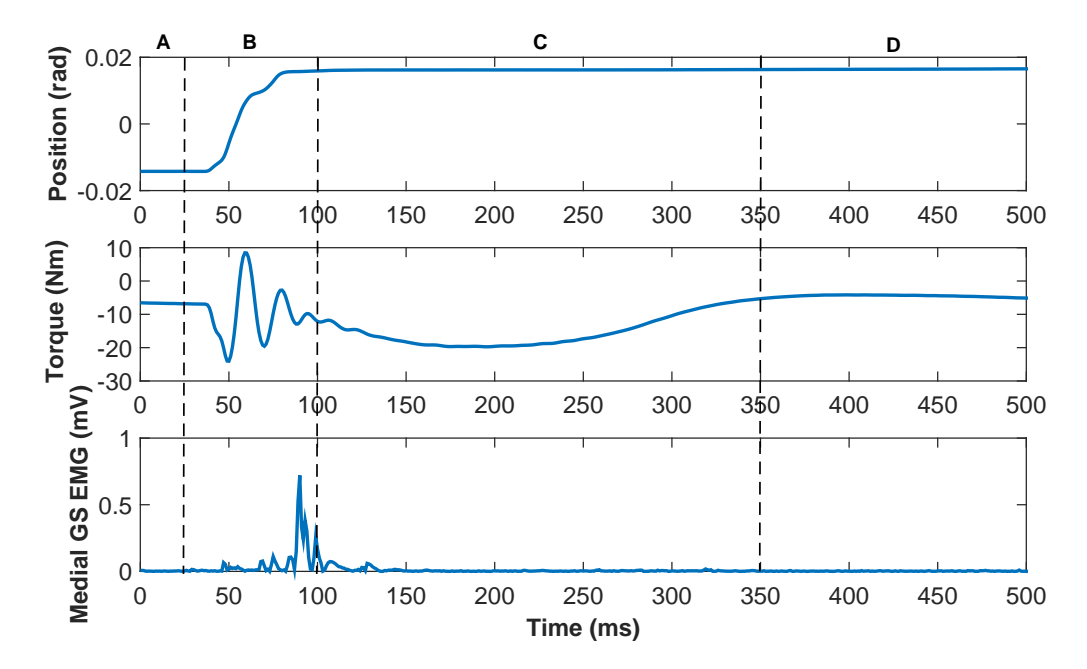


Figure 5–2: Sample subdivided response drawn from a typical experiment. Position is normalized between -5 and 5, and EMG is rectified and normalized between -30 and -15. Peak detected velocity occurs at 50ms. The subsections are as follows: (A) pre-response (0-25ms), (B) intrinsic response (25-100ms), (C) reflex response (100-350ms), (D) post-reflex (350-500ms).

of the reflex region was chosen at the 100ms mark. The reflex torque transient is the result of the low-pass dynamics between an EMG spike and muscle torque generation, and typically lasted for 200-250ms. The EMG background activity for each muscle was calculated as the average of the rectified EMG signal over subsection (A).

As shown in the previous chapter, postural sway torque cannot be modeled based on the whole experimental record, and may contain frequency content past 1 Hz, and potentially up to 2 Hz [60]; therefore, sway torque will be estimated as piecewise linear.

For each response, a linear trend was fitted to the pre-response torque using linear regression. The background torque and its derivative were defined as the intercept and slope of this line. This trend was then extrapolated to the first 100 ms of the response and removed to prevent it from influencing the intrinsic stiffness estimate.

The background torque in the reflex response section was estimated by linear interpolation between the torque values at 100ms and 350ms. This linear trend was subtracted from the torque in the reflex response section. Sample reflex sections with this trend removed are shown in 5–5. These fits are also shown applied to a full response in Figure 5–4. This detrending was performed because it reduced the variance of the estimated reflex gain parameters with little effect the magnitude.

A second order IBK model $(\frac{\theta(s)}{TQ(s)} = \frac{1}{Is^2 + Bs + K})$ was fit to the de-trended torque in the intrinsic response section for responses to perturbations in both directions. The potentiometer signal and its first and second derivative were used in linear regression of the intrinsic torque response. These signals were each smoothed three times with a three-point, zero-phase moving average filter before differentiation. This was performed to smooth out noise caused by differentiation. The fitted value of K represented the intrinsic stiffness and was compared with the critical stiffness, K_{crit} , calculated according to Equations 2.3 and 2.4.

A sample intrinsic fit is shown in Figure 5–3. The overall variance accounted for (VAF) was low, usually around 60-70%. This suggests error in the modeling of the high-variance components of the intrinsic model, namely the damping parameter B

and inertial parameter I. This could be due to the intrinsic dynamics being higher than second order, a recent finding in our laboratory group [61].

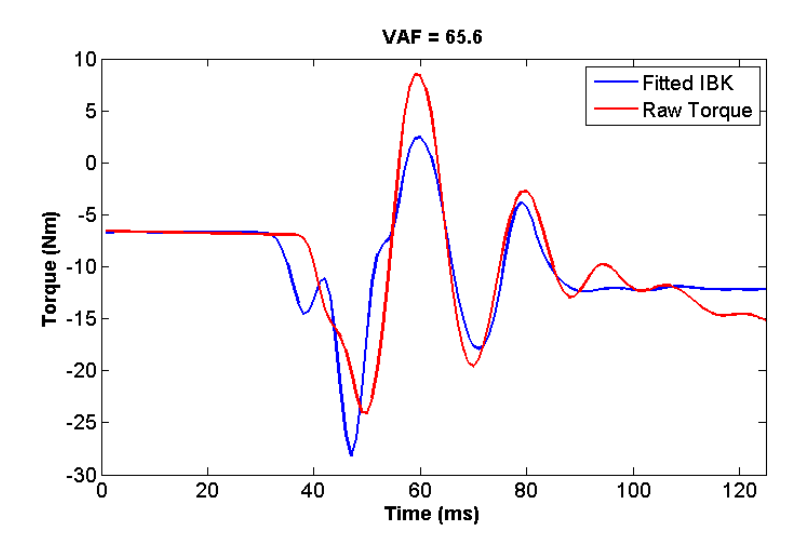


Figure 5–3: Typical IBK model fit to intrinsic torque of a single response. The beginning of the reflex response can be observed toward the end of the window.

Reflex stiffness was modeled as a second order low-pass system in the time domain (see Equation 5.1), derived from the impulse response in the Laplace domain, Equation 2.6. The fitting was done for each dorsiflexing response using MATLAB's curve fitting toolbox.

$$\frac{G\omega_0^2}{\omega_0\sqrt{1-\zeta^2}}e^{-\zeta\omega_0 t}\sin(\omega_0\sqrt{1-\zeta^2 t}+\phi)$$
(5.1)

Reflex fitting was highly accurate, with VAFs of over 95% for strong reflexes. All reflex fits were accepted as valid provided the VAF was greater than 70%. A VAF below 70% was representative of reflex responses which were either very small or nonexistent. This value was determined by trial and error observation of a large

number of fits. Fits with a VAF below the threshold were assigned a gain of zero. Sample reflex fits for strong and weak reflex responses are shown in Figure 5–5.

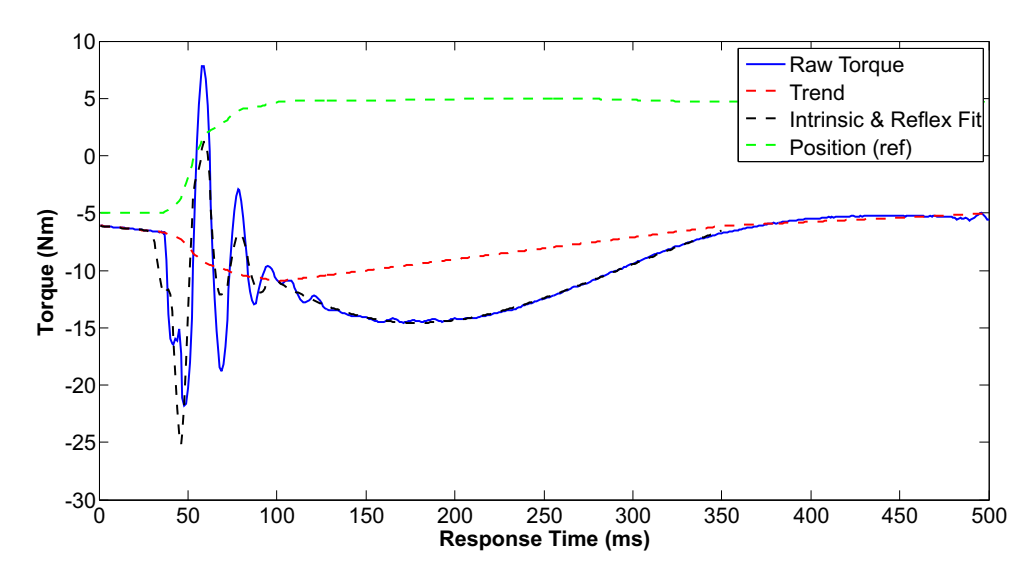


Figure 5–4: Background torque, intrinsic, and reflex fitting for one sample response. The "Trend" line represents the background torques computed from each subsection added to the simulated intrinsic torque based on the estimated intrinsic stiffness value 'K'.

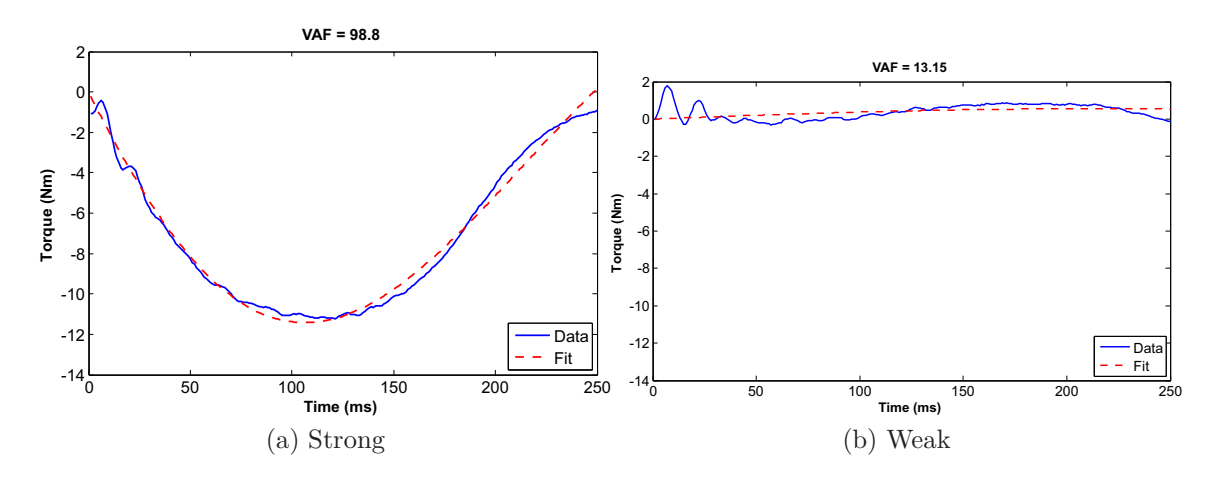


Figure 5–5: Sample reflex fits for strong and weak responses.

Table 5–1: Height, weight, and K_{crit} for each subject.

Subject	Height (cm)	Weight (kg)	K_{crit} (Nm/rad)
1	162	76.2	756.4
2	173	72.6	664.6
3	182	64.2	593.3
4	171	80.0	742.4
5	170	60.8	536.6
6	183	79.4	808.5
7	188	70.4	655.3
8	170	54.3	508.1
9	168	77.8	769.0

The first and last responses from each trial were ignored to avoid using responses that were clipped at the endpoints. Each two-minute trial contained 114 ± 6 responses.

5.2 Results

This section describes the trends observed between intrinsic and reflex stiffness and background torque. The relationship between stiffness and background torque is first presented for one subject and the group results for all nine subjects are then presented. The analyses are based on six two-minute trials acquired for each subject (2 normal, 2 forward-leaning, 2 backward-leaning). The height, weight, and critical stiffness value for each subject are shown in Table 5–1.

Figure 5–6a shows a ten second segment of a typical experimental trial. Postural sway is observable by the changing background torque level throughout the experiment. Intrinsic responses are evident following all changes in position, as evidenced by the spikes in torque. Dorsiflexing (toe-up, such as at 54s) perturbations generated reflex responses that followed the intrinsic responses. Figure 5–6b shows a zoomed-in

view of the raw data. Reflexes and are evidenced by a spike in the medial GS EMG signal (e.g. - slightly before 54.1s) and a dip in torque (e.g. - 54.1s to 54.3s).

Figure 5–7 shows a collection of responses at different background torques. As background torque increases to about 0 Nm, the reflex responses generally become larger. The size of response then decreases again after this point. Changes in the size of the intrinsic response also occurred, although they are not as readily visible in this figure, they will be analyzed in further detail in the next section.

5.2.1 Intrinsic Stiffness

Figures 5–8 and 5–9 show scatter plots of intrinsic stiffness against background torque for all nine subjects. Individual responses are indicated by the dots while the smooth red line is the trend fitted to the data using a moving window median method. For each subject, the intrinsic stiffness values were normalized to the value of critical stiffness. The value of this trend line at any point is equal to the median value of the all points within 5 Nm of background torque. Intrinsic stiffness was smallest near -5 Nm and increased roughly linearly with background torque in either direction.

Figure 5–10 shows the trends of intrinsic stiffness for all subjects. The mean background torque of all responses for each subject is subtracted from each trendline in order to normalize the presentation of the trends for all subjects. Most subjects had a local minimum in intrinsic stiffness or a change in the slope of the trend at approximately 10 Nm. For background torques corresponding to the normal trial

paradigm, the intrinsic stiffness decreased approximately linearly, which was characteristic of all subjects. For all subjects, intrinsic stiffness increased as background torque became more negative (i.e. as the COP moved toward the toes).

Figure 5–11 shows the standard error estimates of 'K' for a single subject calculated by the MATLAB 'lscov' function. The standard error for each response was, for this subject, always below $0.05 \cdot K_{crit}$, and typically remained around $0.03 \cdot K_{crit}$. The two divergent lines are due to differing actuator dynamics between plantarflexing and dorsiflexing perturbations. The estimation error is not insignificant, as can be seen in the dotted red lines. This could be due to the issues described earlier with fitting a second order IBK model to the intrinsic response. However, the trend in the data relative to the size of the errors suggest that the changes in intrinsic stiffness are real.

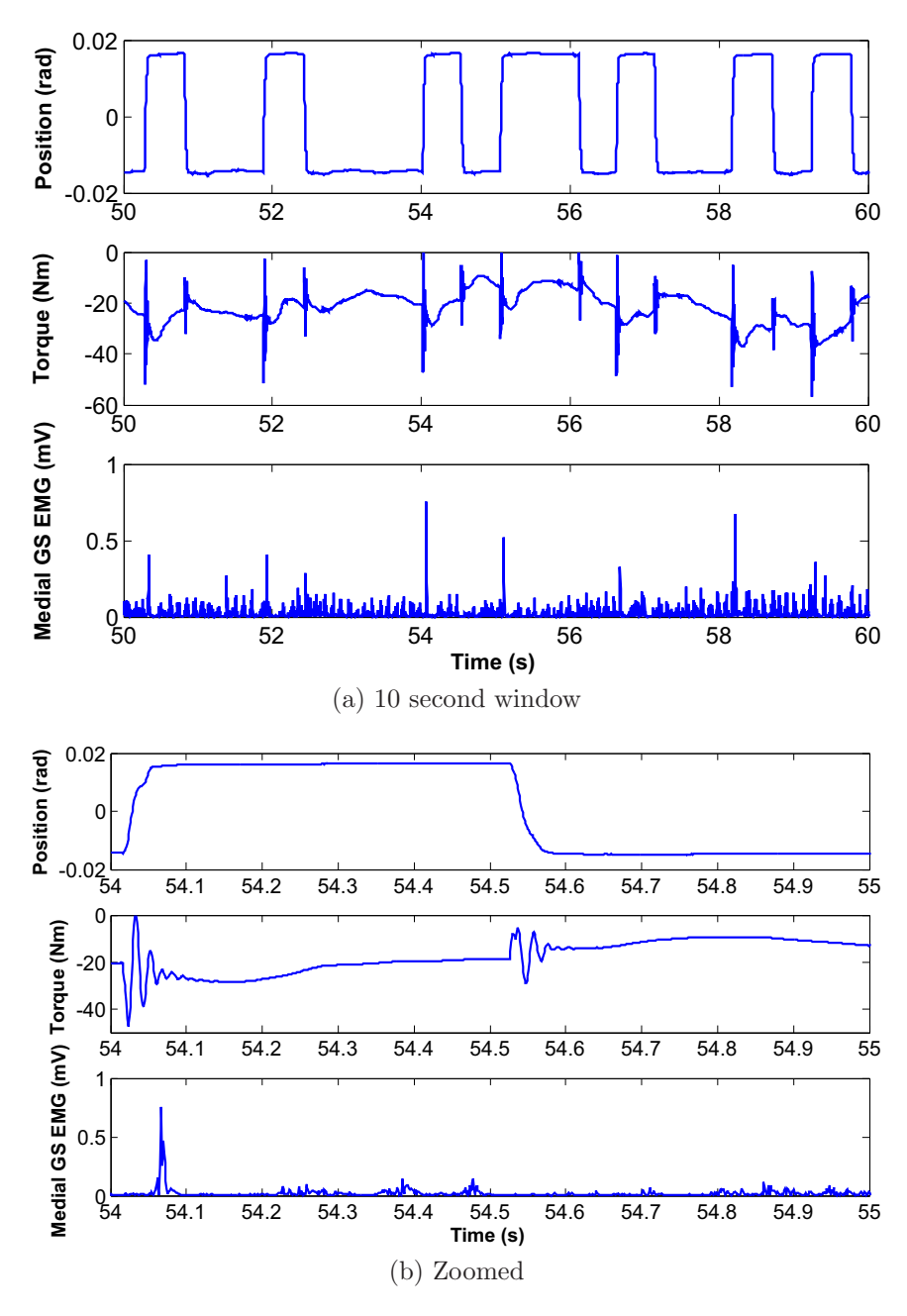


Figure 5–6: Raw data from a forward-leaning trial showing pedal position, torque, and rectified EMG. A positive position indicates a dorsiflexing perturbation, while a negative position indicates a plantarflexing perturbation. Positive torque signified that the subject's weight was centered closer to their heels, while negative torque signified that the subject's weight was centered closer to their toes.

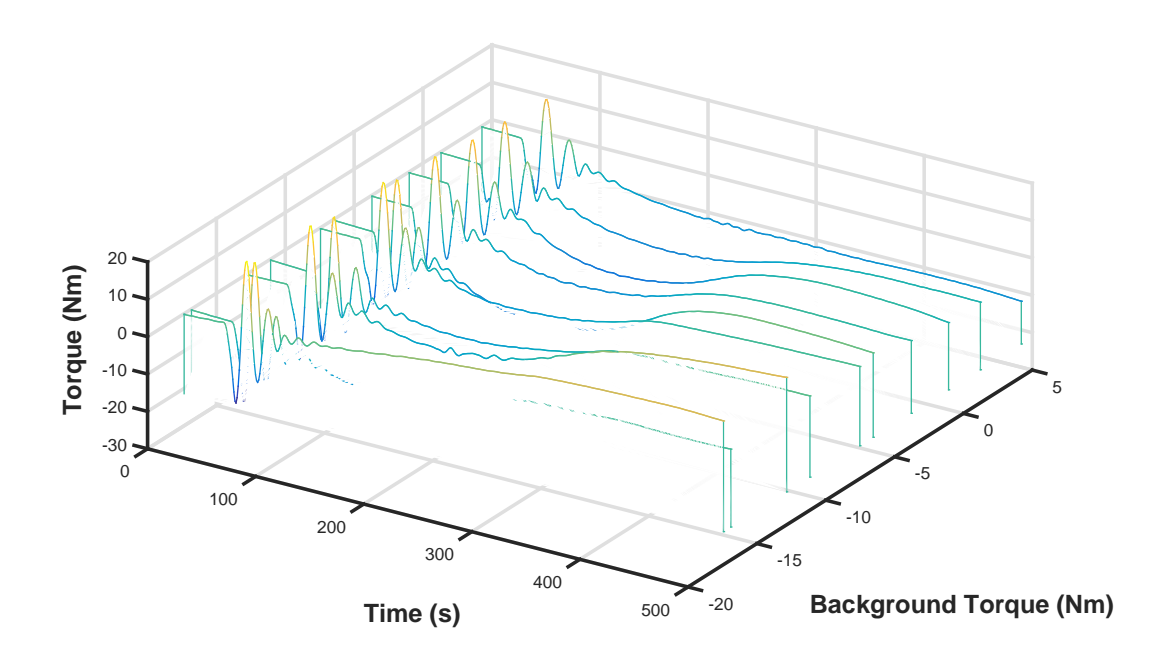


Figure 5–7: Ten individual responses taken from different background torques. Ten groups of equal width in background torque are shown, and a single response was plotted from each group. Group 1 represents the responses with the lowest background torque while group 10 contains the responses with the largest background torque. The background torque value was subtracted from the torque response.

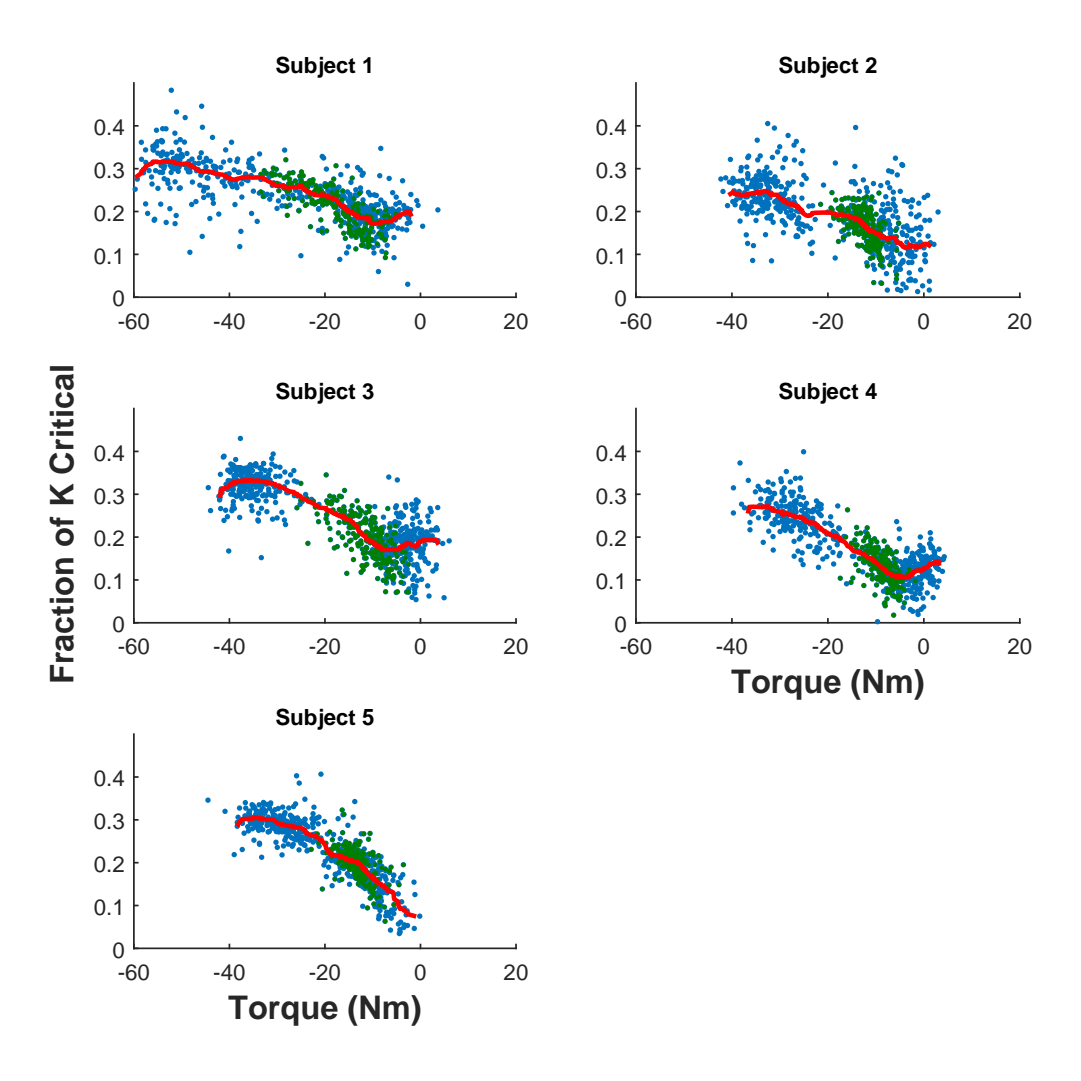


Figure 5–8: Intrinsic stiffness values for all responses from the left leg of subjects 1-5, with a trend line is shown in red. The stiffness is shown as a percentage of the critical value, which was calculated according to Equation 2.3. The green dots represent responses from the normal trial paradigm, while the blue dots represent responses from the leaning trials.

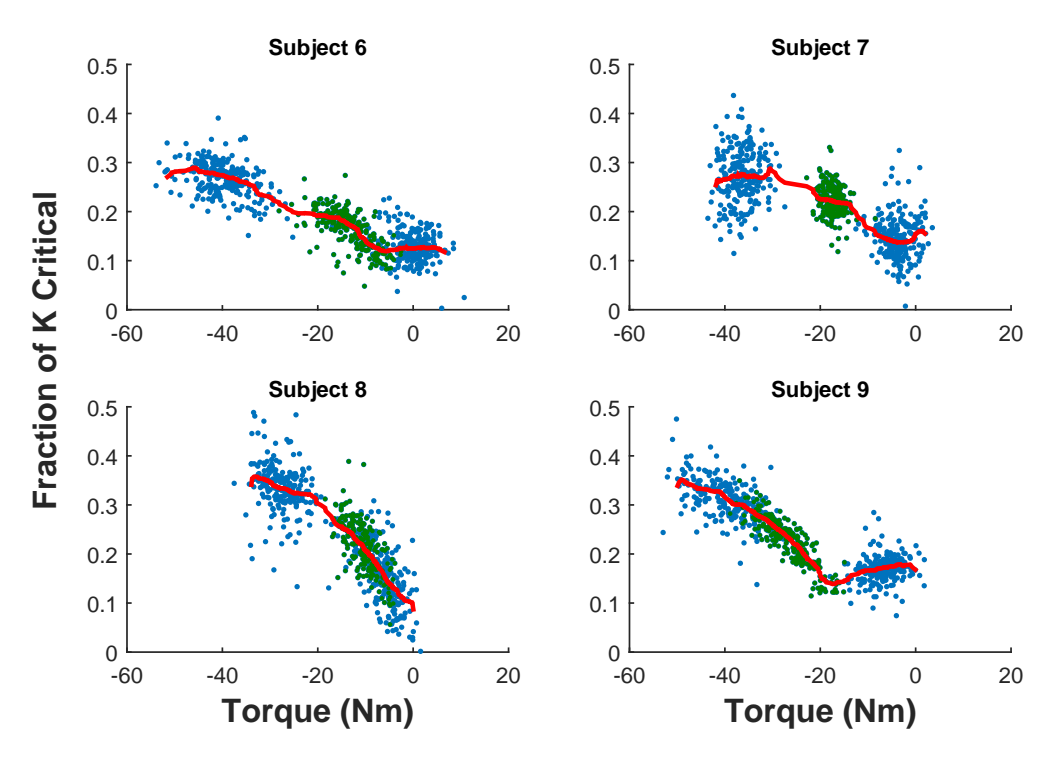


Figure 5–9: Intrinsic stiffness values for all responses from the left leg of subjects 6-9, with a trend line is shown in red. The stiffness is shown as a percentage of the critical value, which was calculated according to Equation 2.3. The green dots represent responses from the normal trial paradigm, while the blue dots represent responses from the leaning trials.

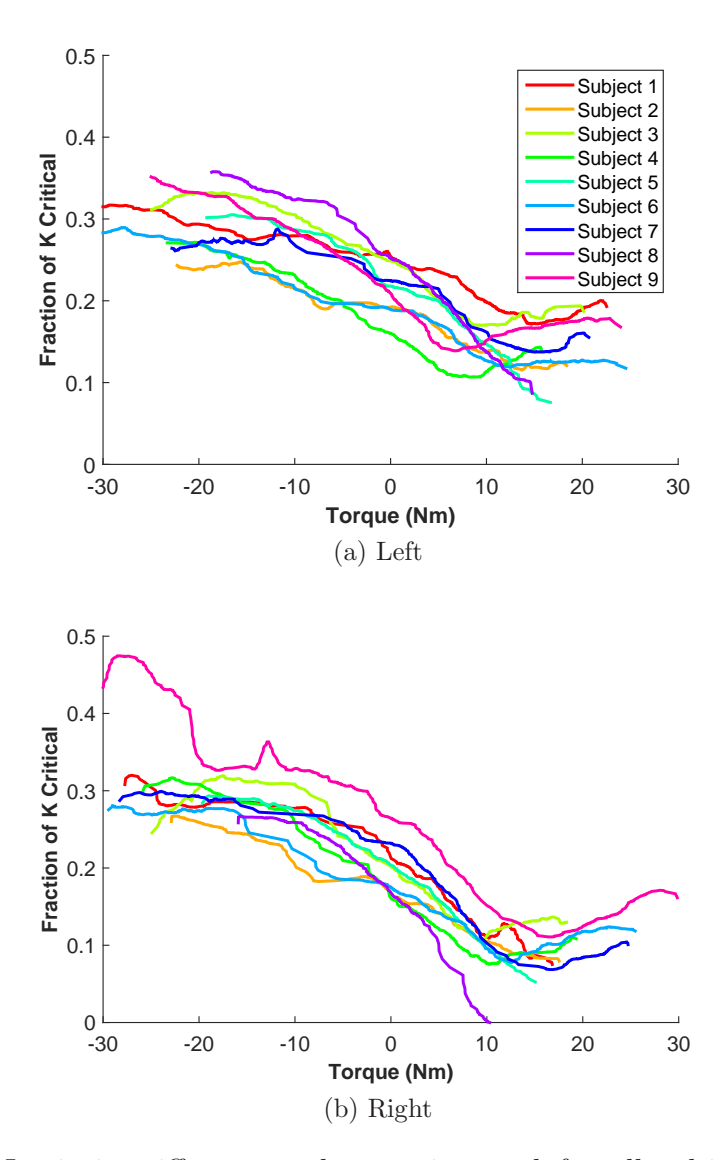


Figure 5–10: Intrinsic stiffness trends superimposed for all subjects. The mean background torque calculated from all responses was subtracted from each trend. Positive torque signified that the subject's weight was centered closer to their heels, while negative torque signified that the subject's weight was centered closer to their toes.

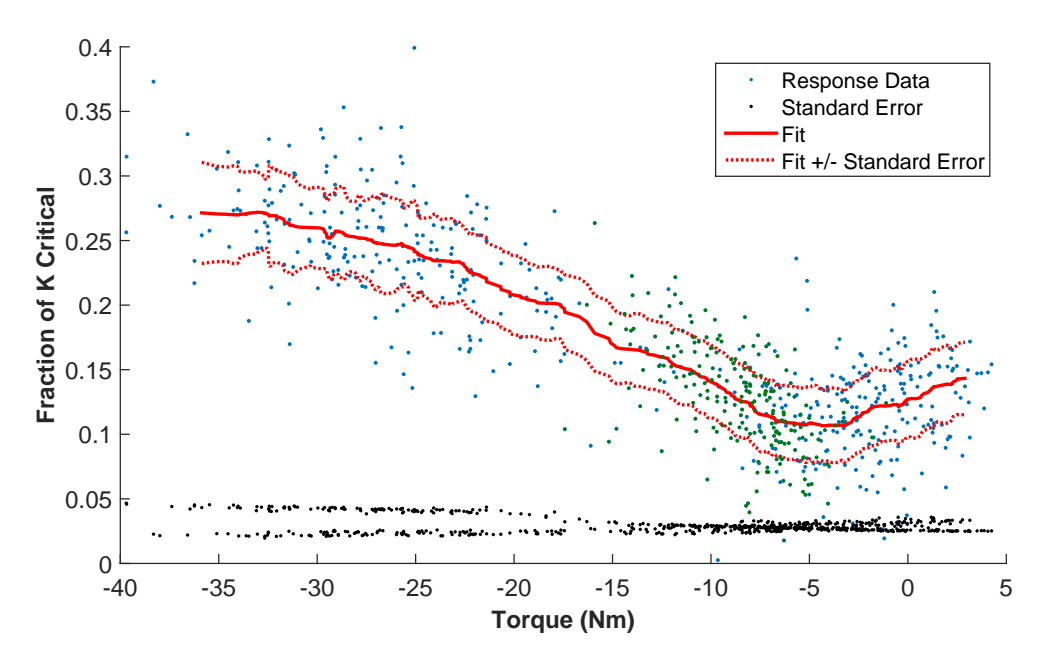


Figure 5–11: Parameter variance estimates for one subject. The standard error of the fitted parameter 'K' is shown for each point. The "Fit +/- Standard Error" lines show the standard error values passed through an averaging filter, then added to and subtracted from the moving window median fit.

5.2.2 Reflex Stiffness

Figure 5–12 shows reflex gain as a function of background torque for the five subjects who exhibited reliable reflex responses. It was greatest near -5 Nm, and decreased to either side. The trend lines were calculated using the same moving window median method used for intrinsic stiffness. Each subject also showed large variability in the size of the reflex responses. Even at background torque values were reflexes tended to be larger, as indicated by the trend line, individual reflex responses were occasionally small or nonexistent.

Figure 5–13 shows the changes in reflex stiffness calculated using a moving window median 10 Nm in width. The mean background torque of all responses for each subject is subtracted from each trendline in order to normalize the presentation of the trends for all subjects. The maximum reflex gain for most subjects occurred near 10 Nm background torque and decreased in either direction. More frequent and larger reflexes occurred for all subjects at a positive background torque, between 5 Nm and 15 Nm. Reflex gain decreased to either side of this maximum for all subjects.

For this section, only responses to dorsiflexing perturbations were considered, since plantarflexing perturbations did not elicit a reflex response. Additionally, subjects 2, 5, 7, and 8 were excluded from the reflex analysis since they had very small reflex responses.

Figure 5–14 shows the 95% confidence interval for the fitted reflex gain from each response for subject 4, which was calculated using the 'confint' function on each individual fit generated by MATLAB's 'fit' command. For this subject, the median 95% confidence interval for all non-zero reflexes was 0.02 Nm s/rad, which

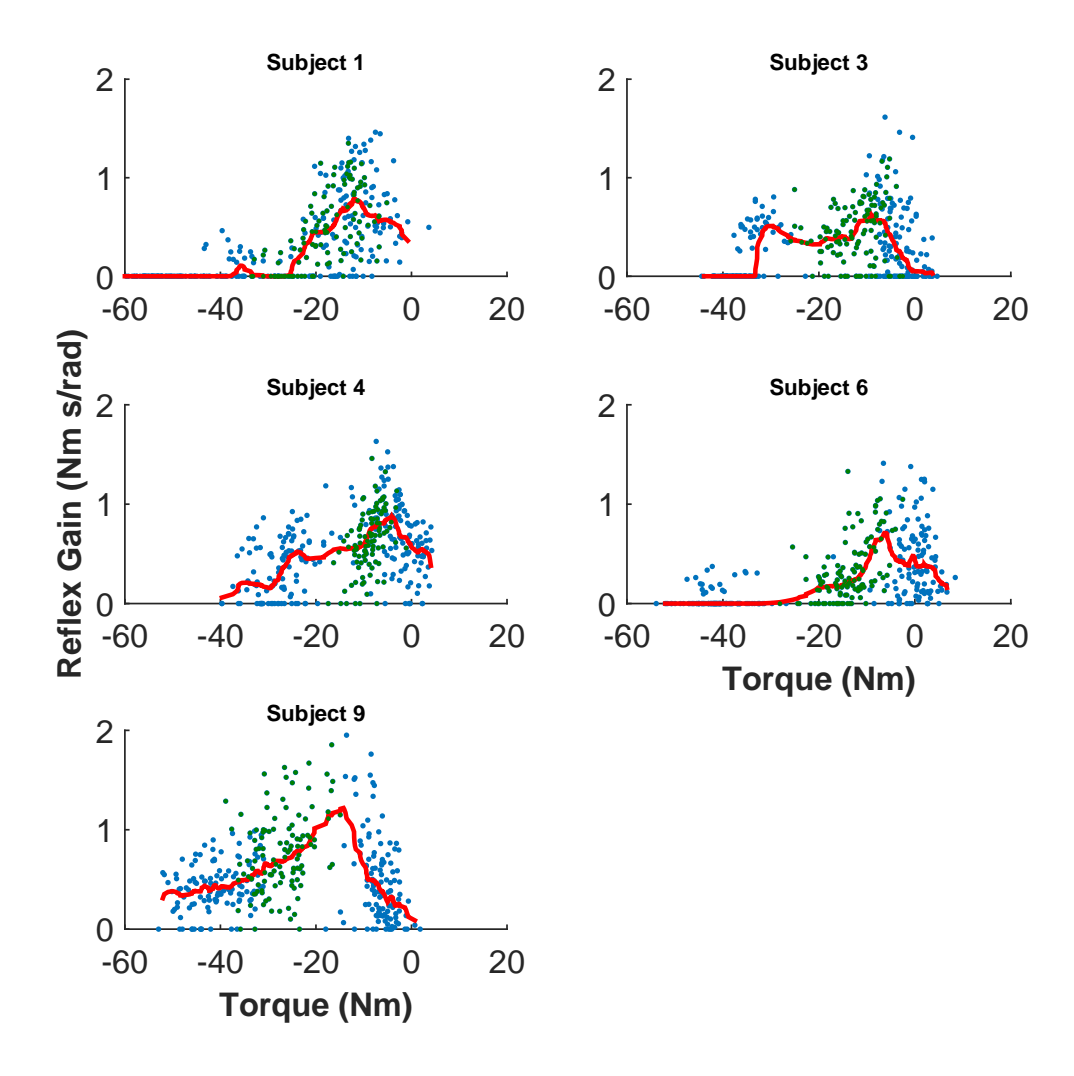


Figure 5–12: Reflex gains for all responses from the left leg of all reflex-displaying subjects. The value of the trend line is the median of the reflex gains of the responses within 5 Nm background torque. The green dots represent responses from the normal trial paradigm, while the blue dots represent responses from the leaning trials.

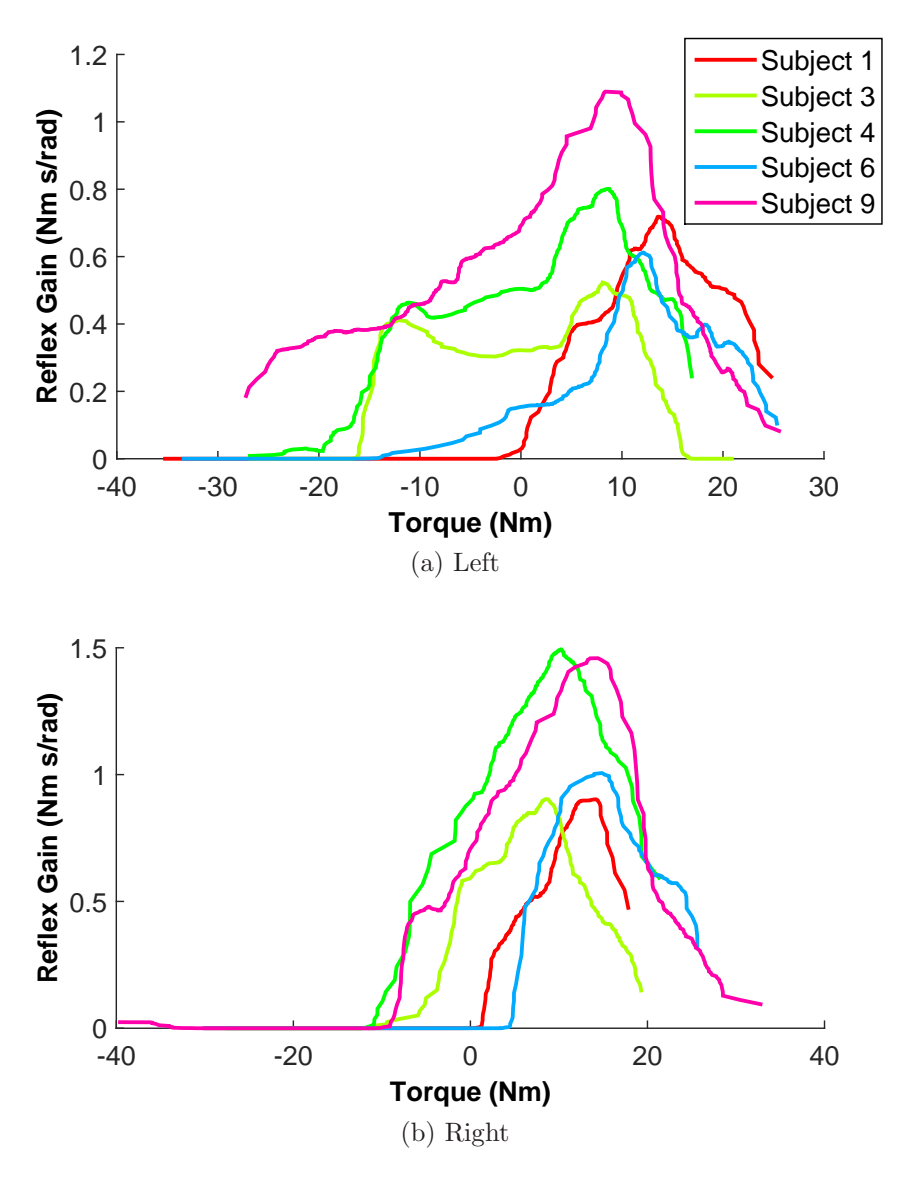
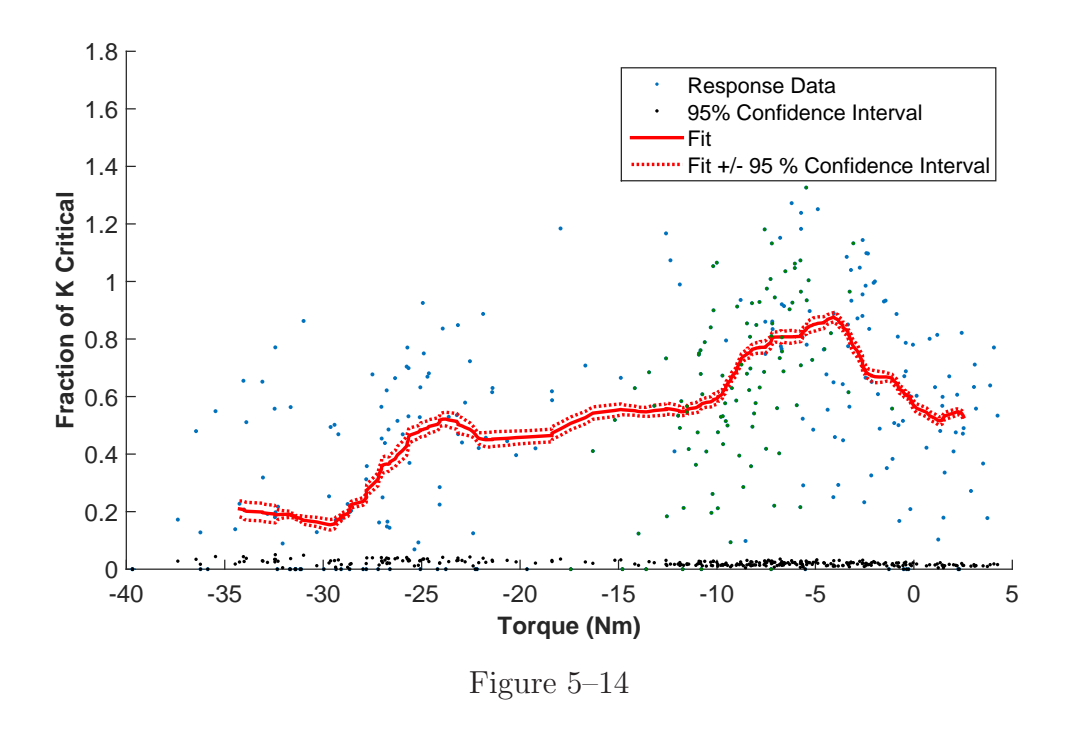


Figure 5–13: Moving window median of reflex gain for subjects exhibiting consistent reflex responses. The mean background torque calculated from all responses was subtracted from each trend.



is small compared to the size of the gains. Other subjects showed similar confidence interval sizes, in some cases larger, but still small compared to the size of the reflex gain. However, while the parametric fitting was accurate, considerable variability was still evident in reflex gain. Furthermore, for most subjects, the distribution of the points within these windows were not Gaussian upon visual examination. These findings strongly suggest that, while background torque is one predictor of reflex gain, there are other factors contributing to its modulation.

5.2.3 EMG Variation

Figure 5–15 shows the relation between initial torque and background EMG, with a trend characterized by the moving median method described in previous sections. This figure most importantly shows that there was great variability in

background muscle activation for the same background torque. For a given level of background activation of any one of the muscles of the lower leg, numerous different background torques were generated. For instance, while the background activation of the medial GS was generally higher at -30 Nm background torque than at 0 Nm, some responses were preceded by very low background activation at both levels. These results suggest that the relative contributions pf each muscle to the joint torque are not fixed, since otherwise we would expect a fairly consistent torque to EMG activation relationship. This variability could also potentially explain some of the variability in the reflex gains. Furthermore, no individual EMG displayed any direct correlation with intrinsic or reflex stiffness.

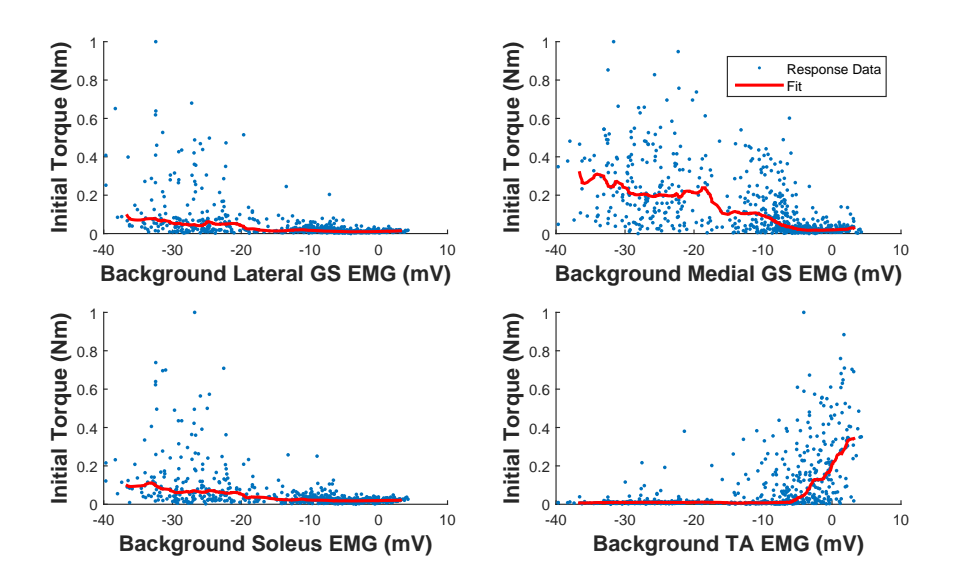


Figure 5–15: Sample distribution of torque versus background muscle activation. Data includes all leaning trials in addition to two normal trials.

Figure 5–16 shows the general variation of the background activity of the lower leg muscles for all subjects, calculated by a moving window median. For most subjects, a larger background activation of the triceps surae muscles generally corresponded to a more negative background torque (COP positioned closer to toes). In regions where the triceps surae muscles were more active, there was less TA muscle activity. Conversely, more positive background torques (COP positioned more over heels) corresponded to a larger background activation of the TA and less triceps surae activation. At background torque values which had minimal EMG activity, this roughly corresponded to the minimum in intrinsic stiffness and maximum in reflex stiffness shown in prior sections. It is important to note that this figure represents only general trends in activity.

5.2.4 Covariation of Intrinsic and Reflex Stiffnesses

Figure 5–17 compares the variation reflex gain and intrinsic stiffness with initial torque. In general, these trends mirror each other in the y-direction. As intrinsic stiffness increases, reflex gain decreases, and vice versa. Also, evident across all subjects exhibiting reflexes, the minimum intrinsic stiffness and maximum reflex gain occur at similar values of background torque.

5.2.5 Feedforward Control

Sway velocity has been proposed as a modulator of reflex gain [5], though no such relationship was demonstrated in this study. Figure 5–18 shows a graph of a typically observed pattern between stiffness and the background torque derivative; no relationship between the two variables is observed in either panel. Although no relationship was evident, given the high variability of intrinsic and reflex responses

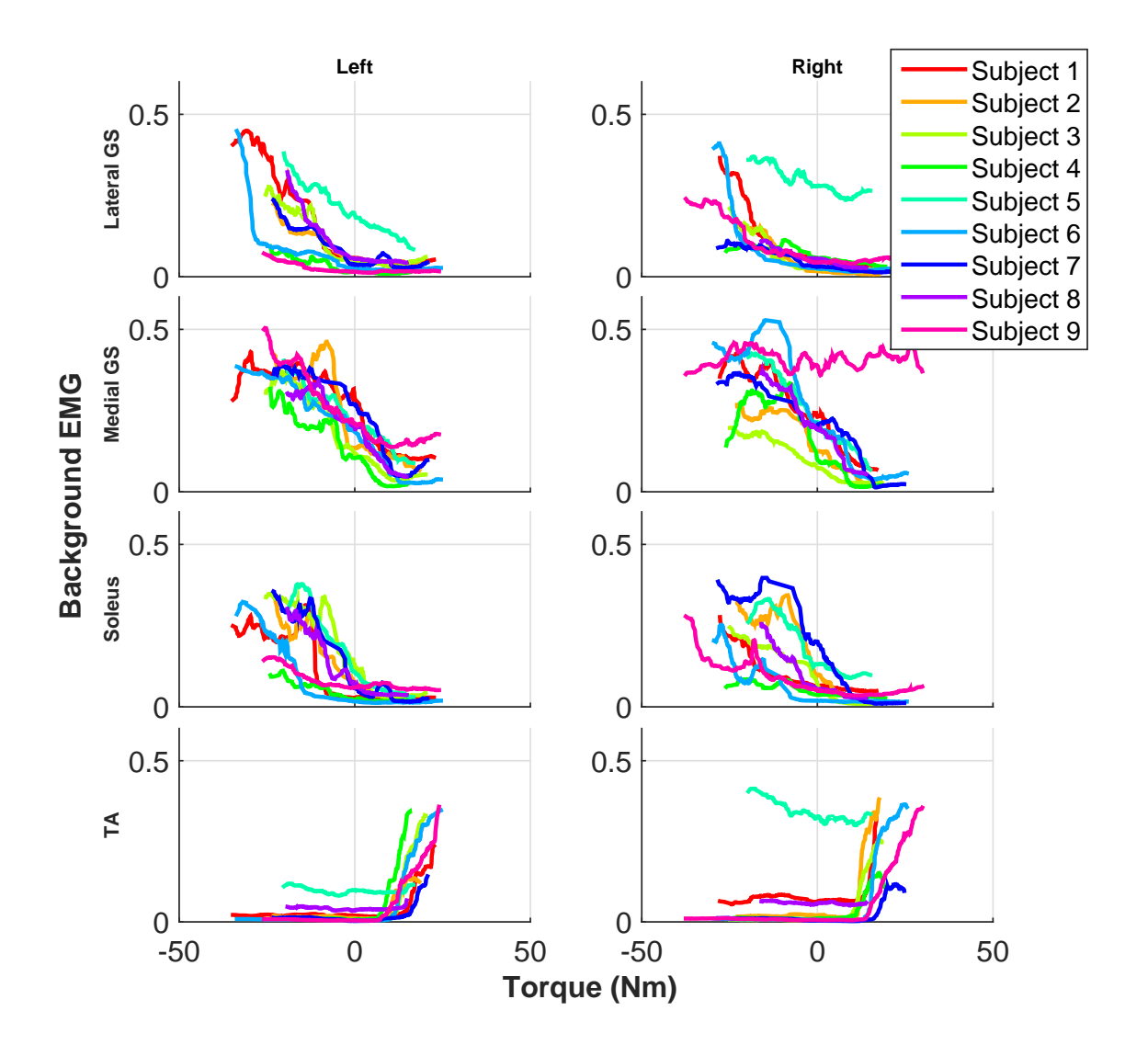


Figure 5–16: EMG activation trends for all subjects for all muscles in leaning bilaterally perturbed trials. EMG for each subject is normalized from 0 to 1 based on the minimum and maximum background activation observed from the collection of all perturbation responses.

seen in previous sections, any contributions from feed-forward mechanisms could be obscured.

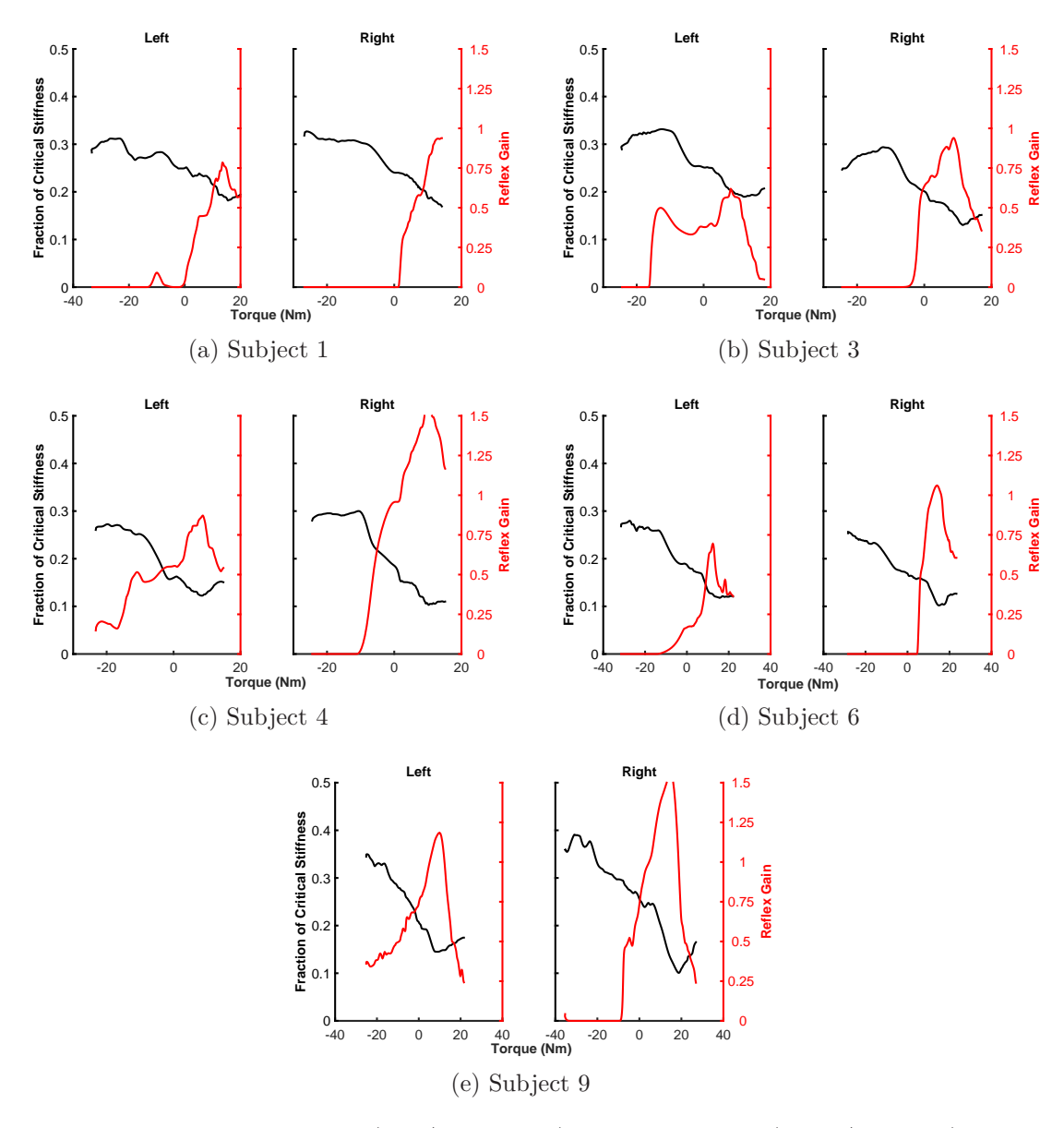


Figure 5–17: Critical stiffness (left/black axis) and reflex gain (right/red axis) superimposed for both legs of the five subjects who displayed reflexes. The curves shown are the moving window median trends displayed in previous sections.

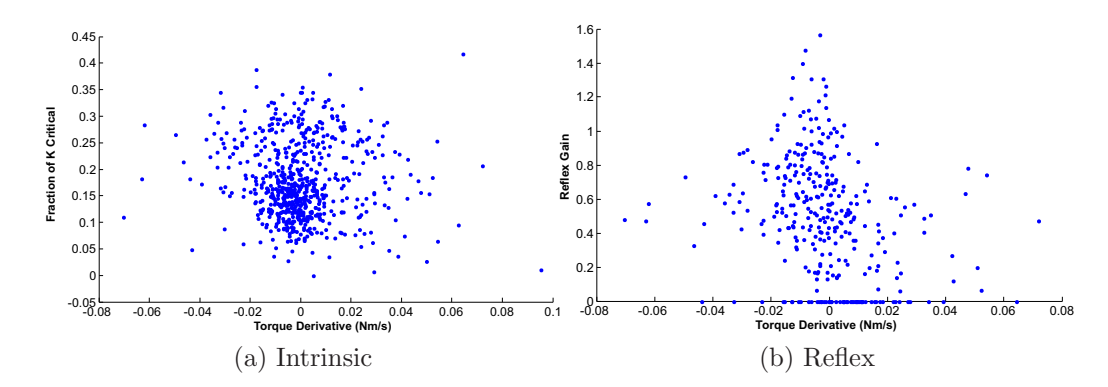


Figure 5–18: Distribution of intrinsic and reflex stiffness versus torque derivative for the left leg of a typical subject. Each blue dot represents one individual response.

5.3 Summary

Intrinsic and reflex stiffness were strongly modulated by postural sway, supporting the view that the CNS intervenes in balance control and sets ankle stiffness. Furthermore, this shows that intrinsic stiffness is not time-invariant. Additionally, the modulation of intrinsic and reflex stiffness were complementary. Intrinsic stiffness was lowest when reflex gain was highest, and vice versa. There was no observable difference in the intrinsic stiffness between subjects who displayed reflexes versus those who didn't. The minimum intrinsic stiffness and maximum reflex stiffness correlated with a net minimum level of background activation of the triceps surae and TA muscles.

CHAPTER 6 Discussion and Conclusions

This study sought to estimate the influence of postural sway on intrinsic and reflex stiffness by examining a large collection of individual responses. Subjects performed several two-minute trials while maintaining quiet stance or a leaning position. The background torque level, intrinsic stiffness, and reflex stiffness were evaluated for each response, and compared amongst one another. The results provide strong evidence for the modulation of dynamic ankle stiffness during perturbed upright stance.

6.1 Modulation of Ankle Stiffness

The primary finding of this study was that the intrinsic stiffness and reflex stiffness varied heavily with postural sway. During normal stance, the reflex torque decreased when the background torque decreased (subject's weight was over the toes), which matches previous results from our lab [5]. This decrease was concurrent with increasing background activity of the triceps surae muscles. Additionally, intrinsic stiffness decreased as subjects swayed backward. This was concurrent with a decrease in the activation level of the triceps surae muscles.

Asking subjects to maintain a forward or backward lean allowed for the evaluation of stiffness for a wider range of background torques. While a linear decrease in intrinsic stiffness with increasing background torque was observed when analyzing normal trials, the leaning paradigm revealed local extremes in intrinsic and reflex stiffness. Intrinsic stiffness increased to each side of a local minimum, while reflex stiffness decreased to either side of a local maximum. The maximum reflex gain corresponded to a minimum intrinsic stiffness, and vice versa. The pattern of trends observed in this experiment were consistent with those observed for supine experiments, in which increasing plantarflexing torque yielded increased intrinsic stiffness and decreased reflex gain when compared to the rest condition [41]. Since intrinsic and reflex stiffness vary heavily with postural sway, their dynamics must be taken fully into account by identification techniques; any analysis method that treats the system as time-invariant will not be able to fully model the dynamics of the system.

In general, reflex and intrinsic gains covaried. When intrinsic stiffness reached a minimum value, reflex gain was at a maximum, and vice versa. These observations suggested a linkage between the control of intrinsic stiffness and reflex gain, and supported the theory for the existence of hybrid control strategies [30, 12].

Subjects tend to prefer to sway about a mean COP location which is slightly in front of the ankle joint [74]. In context with this study and Figures 5–10 and 5–13, this would be at a background torque of 0 Nm. The minimum intrinsic stiffness and maximum reflex gain occur at a torque value that is more positive (closer to the heels) than the mean preferred position; this may represent a state where the COM is directly above the ankle joint.

This observation can be attributed to the control of the inverted pendulum model of upright posture. When the mass of the body is directly above the base of support, the maintenance of stability requires the minimum active intervention compared to any other state. No torque would be theoretically required if there were no external forces and any reactive stabilizing ankle torque would have a maximum effect on the motion of the COM. This is also in agreement with the hypothesis that the postural control system chooses a strategy which minimizes energy expenditure, as a minimum stiffness at the most stable point would minimize unnecessary muscle co-contraction.

Estimates of intrinsic stiffness were generally lower than the critical stiffness value. The stiffness from any leg and any subject typically remained smaller than 45% of critical stiffness. Table 6–1 shows the maximum values from the intrinsic stiffness trends from each leg, which occurred for more negative values of background torque. This table shows that the contribution of intrinsic stiffness from both legs together is, on average, less than 80% of the critical value. However, this does not exclude the possibility that, at certain times, the total intrinsic stiffness may equal or exceed the critical value. Thus, in some cases, intrinsic stiffness is sufficient to stabilize the inverted pendulum, while other scenarios would require the application of active mechanisms.

Table 6–1: Maximum Intrinsic Stiffness $(\frac{K}{K_{crit}})$

Subject	Left	Right	Sum
1	0.32	0.29	0.61
2	0.26	0.26	0.52
3	0.35	0.33	0.67
4	0.28	0.33	0.61
5	0.32	0.31	0.63
6	0.29	0.28	0.57
7	0.29	0.31	0.60
8	0.37	0.28	0.65
9	0.34	0.45	0.80

6.2 Limitations

One concern with removing a mean background torque from each trend line when comparing between subjects in Figures 5–10 and 5–13 is the lack of knowledge of a true equilibrium ankle position for each subject. While the ankles were positioned carefully in line with the actuator axis of rotation, different subjects may position their weight differently at rest (i.e. - the mean COP location may differ). Slight movements of the foot between trials may also affect the consistency of torque readings between trials. These factors suggest that the meaning of mean torque for the responses presented herein is not identical between subjects. We therefore cannot truly tell whether the subject's COM is directly over the ankle when the intrinsic stiffness is at a minimum and reflex is at a maximum. Combining the measures collected here with motion capture data could solve this issue, and add support to the theory that the CNS chooses the strategy which expends the least energy.

The normalization of the EMG between subjects could additionally be improved. To acquire a more accurate measure of background activity during upright standing, a method for measuring something similar to the maximum voluntary contraction (MVC) in standing would be valuable. In supine experiments, this involves asking the subject to exert a strong pushing or pulling force against the actuator. Since subjects in upright experiments are not strapped to the foot pedal, a different method would be required. This could consist of asking the subject to stand on their toes and/or heels to establish the contraction level required to lift his/her weight from the ground. This condition would not be observed when applying small perturbations experimentally, so contraction level would remain well below this measure of MVC at

all times. This would allow for better comparison of EMG activity between subjects. Finally, no relationship between any one EMG signal and intrinsic or reflex gain was observed. This may suggest that the relative contribution of the lower leg muscles to ankle torque changes over time.

A way to predict torque from EMG would be of value in the study of posture. Not only could we then determine the contributions of each muscle to ankle torque, such a method would also provide the ability to predict the postural sway torque using EMG signals, rather than processing it from the output torque itself. If we could reliably estimate postural sway from EMG signals, our estimates of the intrinsic and reflex pathways would improve, and we would be able to remove the sway torque that can compromise the stiffness estimates.

Furthermore, all of the healthy subjects recruited for these experiments were young graduate students, the majority of whom were male. This sample may not be representative of the general population. A wider demographic sampling of healthy subjects could alter the results reached in this study and would strengthen the conclusions drawn.

6.2.1 Variability

The variability of the reflex gains were generally quite large, though the variance of the parameter estimates was comparatively low. This suggests that reflex gain is controlled in other manners aside from solely the background torque level. The variance of the intrinsic parameter estimates was comparatively larger. This is likely related to the possibility that intrinsic dynamics display third order dynamics [61].

Given these observations, the variation of the intrinsic and reflex stiffness parameters about the trend lines is due to a combination of computational noise and biological noise. The biological noise may result from a dependence of each stiffness on other parameters, such as the background torque derivative or EMG activation level. However, no such relationships were observed in this study. Concerning activation level, this may be because the relative contributions of each muscle to ankle torque are not consistent throughout a trial. Also, while sway velocity has been proposed as a control signal in upright stance [5], its effect may be obscured if its contribution is small compared to the biological noise observed. Furthermore, although contralateral responses do contribute to upright stance [3], they were not estimated in this study and could be a source of error.

6.3 Future Work

6.3.1 Modulation of Stiffness

This study presents the estimation of changing ankle dynamics with respect to different set points of postural sway. While some interesting connections between background torque and stiffness were presented, other variables also likely contribute to the modulation of the response. Sway velocity has been proposed as a modulator of reflex gain [5], and there is evidence that body velocity composes a significant portion of the neural motor command controlling quiet stance posture [38]. However, no clear relationship between the sway velocity and stiffness was observed in this study. Additionally, while perturbations were applied about a horizontal pedal position in this study, changes in dynamics resulting from a change in this position set point could be valuable to investigate.

6.3.2 System Identification

The understanding of ankle stiffness during upright stance could additionally be improved by further development and application of nonlinear, time-varying identification techniques to upright stance. Such methods are better equipped to deal with measurement noise and biological noise. These could also improve upon the parallel cascade method by estimating variable dynamics based on a parameter that indicates the changing state, such as postural sway or joint position.

Furthermore, the inclusion of a method which can accurately predict sway torque would assist in the isolation of intrinsic and reflex dynamics. When postural sway is estimated by low-pass filtering raw torque, the estimates of the dynamics can become biased in the presence of reflexes and perturbations. A piecewise-linear signal, similar to the method described in the previous section, could be created for periods of data containing perturbations and reflexes. The raw torque outside these periods could be left unaltered. This combination of signals could subsequently low-pass filtered, yielding a smooth estimate of sway torque. Alternatively, an identification method could model postural sway torque from EMG. Finding a way of appropriately estimating this signal would allow us to isolate it and prevent its influence on intrinsic and reflex torque. Furthermore, it would give us a way to estimate the state of the system and identify the effect of the different states on ankle stiffness.

6.3.3 Contralateral Mechanisms

While contralateral torque responses were observed in the preceding experiments, their effects on intrinsic and reflex stiffness were not examined. Previous lab work indicated an improvement in the prediction of output torque when an additional contralateral identification pathway was included alongside the parallel cascade identification [3]. This could have contributed to some of the variance in the parameter estimates in this work.

Future studies could benefit from the design of an input which allows a contralateral torque response to be repeatably measured without obfuscation by ipsilateral intrinsic or reflex responses. Conversely, an input could be designed such that contralateral responses would not interfere with the estimation of ipsilateral stiffness. Either goal could be accomplished by timing the left and right perturbations such that they do not occur too near one another (i.e. - the responses are allowed to dissipate before another perturbation occurs).

6.3.4 Sensory Contributions to Stiffness

While visual, vestibular, and proprioceptive signals have been shown to contribute to the control of balance, none of their contributions were explicitly explored in this study. Future experiments could evaluate the change in the intrinsic and reflex parameters for trials in which subjects would stand with their eyes closed or would be subjected to additional body weight. This would serve to reduce or alter the sensory information received and processed by the CNS. These results could be related to the findings presented in this study in order to understand the relative contributions of changing sensory feedback.

6.4 Conclusions

This thesis sought to understand the modulation of ankle joint stiffness with changing postural sway. This was undertaken by evaluating the responses resulting from position perturbations applied at the ankle. Each experiment was divided into a collection of individual responses, which were then quantified and parameterized.

Intrinsic and reflex stiffness were modulated heavily by postural sway. Neither parameter can be appropriately modeled as stationary during upright stance. These changes in stiffness were amplified when subjects were asked to lean forward and backward. This allowed for observation of stiffness dynamics over a wider range of background torque than normal quiet stance trials alone.

The modulation of intrinsic and reflex stiffness were also complementary. Intrinsic gain was highest when reflex gain was lowest, and vice versa. Local extrema of intrinsic and reflex stiffness were associated with a net minimum level of background activation of the triceps surae and TA muscles. Subjects additionally tend to prefer to sway about a mean COP location which is slightly in front of the ankle joint [74], which suggests that these extrema correspond to a COM position located directly above the ankle. These observations are in agreement with the hypothesis that the postural control system chooses a strategy which minimizes energy expenditure, as a minimum stiffness at the most stable point would minimize unnecessary muscle co-contraction.

These results highlight the need for an identification method that can fully encompass the time-varying complexity of upright stance. Furthermore, while this research increases the understanding of the modulation of ankle stiffness dynamics, much more study is required before a full and accurate model of postural control can exist.

References

- [1] Anthropometry and biomechanics. [cited 2014; from http://msis.jsc.nasa.gov/sections/section03.htm]. NASA-STD-3000.
- [2] Lower leg muscles. [cited 2014; adapted from http://web.uaccb.edu/academicdivisions/mathscience/science/bwheeler/ess/figs/06 20figure-u.jpg]. © 2009 Pearson Education, Inc.
- [3] Ferryl Alley. Dynamic ankle stiffness during upright standing. Master's thesis, McGill University, 2012.
- [4] F Owen Black, Conrad Wall, and Lewis M Nashner. Effects of visual and support surface orientation references upon postural control in vestibular deficient subjects. *Acta oto-laryngologica*, 95(1-4):199–210, 1983.
- [5] P.J. Bock and R.E. Kearney. Modulation of stretch reflex excitability during quiet human standing. *Proceedings of the 26th Annual International Conference of the IEEE Engineering in Medicine and Biology Society, Vols 1-7*, 26(1):4684–4687, 2004.
- [6] RR Carter, PE Crago, and MW Keith. Stiffness regulation by reflex action in the normal human hand. *Journal of neurophysiology*, 64(1):105–118, 1990.
- [7] Maura Casadio, Pietro G Morasso, and Vittorio Sanguineti. Direct measurement of ankle stiffness during quiet standing: implications for control modelling and clinical application. *Gait & posture*, 21(4):410–424, 2005.
- [8] Robert Creath, Tim Kiemel, Fay Horak, Robert Peterka, and John Jeka. A unified view of quiet and perturbed stance: simultaneous co-existing excitable modes. *Neuroscience letters*, 377(2):75–80, 2005.
- [9] V. Dietz, G.A. Horstmann, and W. Berger. Interlimb coordination of leg-muscle activation during perturbation of stance in humans. *Journal of neurophysiology*, 62(3):680–693, 1989.

- [10] VOLKER Dietz. Human neuronal control of automatic functional movements: interaction between central programs and afferent input. *Physiological reviews*, 72(1):33–69, 1992.
- [11] RC Fitzpatrick, JL Taylor, and DI McCloskey. Ankle stiffness of standing humans in response to imperceptible perturbation: reflex and task-dependent components. *The Journal of physiology*, 454(1):533–547, 1992.
- [12] Richard Fitzpatrick, David Burke, and Simon C Gandevia. Loop gain of reflexes controlling human standing measured with the use of postural and vestibular disturbances. *Journal of Neurophysiology*, 76(6):3994–4008, 1996.
- [13] S.M. Forster, R. Wagner, and R.E. Kearney. A bilateral electro-hydraulic actuator system to measure dynamic ankle joint stiffness during upright human stance. In *Engineering in Medicine and Biology Society*, 2003. Proceedings of the 25th Annual International Conference of the IEEE, volume 2, pages 1507–1510. IEEE, 2003.
- [14] William H Gage, David A Winter, James S Frank, and Allan L Adkin. Kinematic and kinetic validity of the inverted pendulum model in quiet standing. *Gait & posture*, 19(2):124–132, 2004.
- [15] Plamen Gatev, Sherry Thomas, Thomas Kepple, and Mark Hallett. Feedforward ankle strategy of balance during quiet stance in adults. *The Journal of physiology*, 514(3):915–928, 1999.
- [16] Michael Günther, Sten Grimmer, Tobias Siebert, and Reinhard Blickhan. All leg joints contribute to quiet human stance: A mechanical analysis. *Journal of biomechanics*, 42(16):2739–2746, 2009.
- [17] Michael Günther, Otto Müller, and Reinhard Blickhan. Watching quiet human stance to shake off its straitjacket. *Archive of Applied Mechanics*, 81(3):283–302, 2011.
- [18] C Guyton Arthur and E Hall Jhon. *Textbook of medical physiology*. Prism Books Pvt Limited, 1996.
- [19] Fay B Horak, Gammon M Earhart, and Volker Dietz. Postural responses to combinations of head and body displacements: vestibular-somatosensory interactions. *Experimental brain research*, 141(3):410–414, 2001.

- [20] Fay B Horak and Lewis M Nashner. Central programming of postural movements: adaptation to altered support-surface configurations. *Journal of neuro-physiology*, 55(6):1369–1381, 1986.
- [21] C. Hunt. Mammalian muscle spindle: peripheral mechanisms. *Physiological reviews*, 70(3):643–663, 1990.
- [22] R.E. Isman and V.T. Inman. Anthropometric studies of the human foot and ankle. *Bulletin of Prosthetics Research*, pages 97–129, 1969.
- [23] Kian Jalaleddini, Ferryl Alley, and Robert Edward Kearney. Identification of hammerstein systems from short segments of data: Application to stretch reflex identification. In *System Identification*, volume 16, pages 798–803, 2012.
- [24] L. Jami. Golgi tendon organs in mammalian skeletal muscle: functional properties and central actions. *Physiological Reviews*, 72(3):623–666, 1992.
- [25] John Jeka, Kelvin Oie, Gregor Schöner, Tjeerd Dijkstra, and Elaine Henson. Position and velocity coupling of postural sway to somatosensory drive. *Journal of Neurophysiology*, 79(4):1661–1674, 1998.
- [26] John J Jeka and James R Lackner. The role of haptic cues from rough and slippery surfaces in human postural control. *Experimental Brain Research*, 103(2):267–276, 1995.
- [27] R.E. Kearney and I.W. Hunter. System identification of human triceps surae stretch reflex dynamics. *Experimental Brain Research*, 51(1):117–127, 1983.
- [28] R.E. Kearney and I.W. Hunter. Nonlinear identification of stretch reflex dynamics. *Annals of biomedical engineering*, 16(1):79–94, 1988.
- [29] R.E. Kearney and I.W. Hunter. System identification of human joint dynamics. Critical reviews in biomedical engineering, 18(1):55–87, 1990.
- [30] R.E. Kearney, R.B. Stein, and L. Parameswaran. Identification of intrinsic and reflex contributions to human ankle stiffness dynamics. *Biomedical Engineering*, *IEEE Transactions on*, 44(6):493–504, 1997.
- [31] Tim Kiemel, Alexander J Elahi, and John J Jeka. Identification of the plant for upright stance in humans: multiple movement patterns from a single neural strategy. *Journal of neurophysiology*, 100(6):3394–3406, 2008.

- [32] T. Ledin, P.A. Fransson, and M. Magnusson. Effects of postural disturbances with fatigued triceps surae muscles or with 20% additional body weight. *Gait & posture*, 19(2):184–193, 2004.
- [33] Ian D Loram, Sue M Kelly, and Martin Lakie. Human balancing of an inverted pendulum: is sway size controlled by ankle impedance? *The Journal of physiology*, 532(3):879–891, 2001.
- [34] Ian D Loram and Martin Lakie. Direct measurement of human ankle stiffness during quiet standing: the intrinsic mechanical stiffness is insufficient for stability. The journal of physiology, 545(3):1041–1053, 2002.
- [35] Ian D Loram, Constantinos N Maganaris, and Martin Lakie. Human postural sway results from frequent, ballistic bias impulses by soleus and gastrocnemius. *The Journal of physiology*, 564(1):295–311, 2005.
- [36] D. Ludvig, I. Cathers, and R.E. Kearney. Voluntary modulation of human stretch reflexes. *Experimental Brain Research*, 183(2):201–213, 2007.
- [37] Kei Masani, Milos R Popovic, Kimitaka Nakazawa, Motoki Kouzaki, and Daichi Nozaki. Importance of body sway velocity information in controlling ankle extensor activities during quiet stance. *Journal of Neurophysiology*, 90(6):3774–3782, 2003.
- [38] Kei Masani, Albert H Vette, Masaki O Abe, and Kimitaka Nakazawa. Center of pressure velocity reflects body acceleration rather than body velocity during quiet standing. *Gait & Posture*, 2013.
- [39] Kei Masani, Albert H Vette, and Milos R Popovic. Controlling balance during quiet standing: proportional and derivative controller generates preceding motor command to body sway position observed in experiments. *Gait & posture*, 23(2):164–172, 2006.
- [40] T.A. McMahon. *Muscles, Reflexes, and Locomotion*. Princeton paperbacks. Princeton University Press, 1984.
- [41] M.M. Mirbagheri, H. Barbeau, and R.E. Kearney. Intrinsic and reflex contributions to human ankle stiffness: variation with activation level and position. *Experimental Brain Research*, 135(4):423–436, 2000.
- [42] MM Mirbagheri, RE Kearney, H Barbeau, and M Ladouceur. Parametric modeling of the reflex contribution to dynamic ankle stiffness in normal and spinal

- cord injured spastic subjects. In Engineering in Medicine and Biology Society, 1995., IEEE 17th Annual Conference, volume 2, pages 1241–1242. IEEE, 1995.
- [43] G Mochizuki, John Gregory Semmler, TD Ivanova, and SJ Garland. Low-frequency common modulation of soleus motor unit discharge is enhanced during postural control in humans. *Experimental brain research*, 175(4):584–595, 2006.
- [44] Keith L Moore, Arthur F Dalley, and Anne MR Agur. Clinically Oriented Anatomy. Lippincott Williams & Wilkins, 2006.
- [45] Pietro G Morasso and Vittorio Sanguineti. Ankle muscle stiffness alone cannot stabilize balance during quiet standing. *Journal of Neurophysiology*, 88(4):2157–2162, 2002.
- [46] Pietro G Morasso and Marco Schieppati. Can muscle stiffness alone stabilize upright standing? *Journal of Neurophysiology*, 82(3):1622–1626, 1999.
- [47] BE Moyer, MS Redfern, and R Cham. Biomechanics of trailing leg response to slipping-evidence of interlimb and intralimb coordination. *Gait & posture*, 29(4):565–570, 2009.
- [48] Lewis M Nashner. Adaptation of human movement to altered environments. Trends in Neurosciences, 5:358–361, 1982.
- [49] Lewis M Nashner, F Owen Black, CIII Wall, et al. Adaptation to altered support and visual conditions during stance: patients with vestibular deficits. *The Journal of Neuroscience*, 2(5):536–544, 1982.
- [50] LM Nashner. Adapting reflexes controlling the human posture. Experimental Brain Research, 26(1):59–72, 1976.
- [51] Sukyung Park, Fay B Horak, and Arthur D Kuo. Postural feedback responses scale with biomechanical constraints in human standing. *Experimental Brain Research*, 154(4):417–427, 2004.
- [52] RJ Peterka. Sensorimotor integration in human postural control. *Journal of neurophysiology*, 88(3):1097–1118, 2002.
- [53] Robert J Peterka and Patrick J Loughlin. Dynamic regulation of sensorimotor integration in human postural control. *Journal of Neurophysiology*, 91(1):410– 423, 2004.

- [54] P.F Polastri, J.A. Barela, T. Kiemel, and J.J. Jeka. Dynamics of inter-modality re-weighting during human postural control. *Experimental Brain Research*, 223(1):99–108, 2012.
- [55] REKLAB. Reklab online manual [cited 2013; http://www.bme.mcgill.ca/reklab/manual/]. 2006.
- [56] David A Rosenbaum. *Human motor control*. San Diego: Academic Press Inc., 1991.
- [57] N. Sarabon, J. Rosker, S. Loefler, and H. Kern. The effect of vision elimination during quiet stance tasks with different feet positions. *Gait & posture*, 2013.
- [58] J.P. Scholz and S.K. Campbell. Muscle spindles and the regulation of movement. *Physical Therapy*, 60(11):1416–1424, 1980.
- [59] D.U. Silverthorn. *Human Physiology*. San Francisco: Pearson Education Inc., 2007.
- [60] R.W. Soames and J. Atha. The spectral characteristics of postural sway behaviour. European Journal of Applied Physiology and Occupational Physiology, 49(2):169–177, 1982.
- [61] Ehsan Sobhani Tehrani, Kian Jalaleddini, and Robert E. Kearney. Identification of ankle joint stiffness during passive movements a subspace linear parameter varying approach (to appear). Proceedings of 36th Annual International Conference of the IEEE Engineering in Medicine and Biology Society.
- [62] Healthwise Staff. Bones of the ankle joint: Side view. [cited 2014; adapted from https://myhealth.alberta.ca/health/healthy-living/pages/conditions.aspx?hwid=zm2472]. 2012.
- [63] RB Stein and RE Kearney. Nonlinear behavior of muscle reflexes at the human ankle joint. *Journal of neurophysiology*, 73(1):65–72, 1995.
- [64] Richard B Stein and Charles Capaday. The modulation of human reflexes during functional motor tasks. *Trends in neurosciences*, 11(7):328–332, 1988.
- [65] Cynthia Thompson, Marc Bélanger, and Joyce Fung. Effects of plantar cutaneomuscular and tendon vibration on posture and balance during quiet and perturbed stance. *Human movement science*, 30(2):153–171, 2011.

- [66] Egon Toft, Thomas Sinkjær, Steen Andreassen, and KNUD Larsen. Mechanical and electromyographic responses to stretch of the human ankle extensors. *Journal of neurophysiology*, 65(6):1402–1410, 1991.
- [67] Meagan J Warnica, Tyler B Weaver, Stephen D Prentice, and Andrew C Laing. The influence of ankle muscle activation on postural sway during quiet stance. *Gait & Posture*, 2014.
- [68] PL Weiss, IW Hunter, and RE Kearney. Human ankle joint stiffness over the full range of muscle activation levels. *Journal of biomechanics*, 21(7):539–544, 1988.
- [69] P.L. Weiss, R.E. Kearney, and I.W. Hunter. Position dependence of ankle joint dynamicsi. passive mechanics. *Journal of biomechanics*, 19(9):727–735, 1986.
- [70] P.L. Weiss, R.E. Kearney, and I.W. Hunter. Position dependence of ankle joint dynamicsii. active mechanics. *Journal of biomechanics*, 19(9):737–751, 1986.
- [71] D.A. Winter, A.E. Patla, F. Prince, M. Ishac, and K. Gielo-Perczak. Stiffness control of balance in quiet standing. *Journal of Neurophysiology*, 80(3):1211– 1221, 1998.
- [72] D.A. Winter, F. Prince, P. Stergiou, and C. Powell. Medial-lateral and anterior-posterior motor-responses associated with center of pressure changes in quiet standing. *Neuroscience Research Communications*, 12(3):141–148, 1993.
- [73] David A Winter, Aftab E Patla, Milad Ishac, and William H Gage. Motor mechanisms of balance during quiet standing. *Journal of Electromyography and Kinesiology*, 13(1):49–56, 2003.
- [74] David A. Winter, Aftab E. Patla, Shirley Rietdyk, and Milad G. Ishac. Ankle muscle stiffness in the control of balance during quiet standing. *Journal of Neurophysiology*, 85(6):2630–2633, 2001.
- [75] David A Winter, Francois Prince, JS Frank, Corrie Powell, and Karl F Zabjek. Unified theory regarding a/p and m/l balance in quiet stance. *Journal of Neurophysiology*, 75(6):2334–2343, 1996.